Lawrence Berkeley National Laboratory
LBL Dissertations

Title

ELECTRON CAPTURE AND THE AUGER EFFECT IN THE HEAVIEST ELEMENTS

Permalink

https://escholarship.org/uc/item/47h087z3

Author

Gray, Peter Rygaard.

Publication Date

1955-08-01

Thesis/dissertation

eScholarship.org Powered by the California Digital Library
University of California

UCRL 3104

UNIVERSITY OF CALIFORNIA

Radiation Laboratory

TWO-WEEK LOAN COPY

This is a Library Circulating Copy which may be borrowed for two weeks. For a personal retention copy, call Tech. Info. Division, Ext. 5545

BERKELEY, CALIFORNIA

DISCLAIMER

This document was prepared as an account of work sponsored by the United States Government. While this document is believed to contain correct information, neither the United States Government nor any agency thereof, nor the Regents of the University of California, nor any of their employees, makes any warranty, express or implied, or assumes any legal responsibility for the accuracy, completeness, or usefulness of any information, apparatus, product, or process disclosed, or represents that its use would not infringe privately owned rights. Reference herein to any specific commercial product, process, or service by its trade name, trademark, manufacturer, or otherwise, does not necessarily constitute or imply its endorsement, recommendation, or favoring by the United States Government or any agency thereof, or the Regents of the University of California. The views and opinions of authors expressed herein do not necessarily state or reflect those of the United States Government or any agency thereof or the Regents of the University of California.

UCRL-3104

UNIVERSITY OF CALIFORNIA
Radiation Laboratory
Berkeley, California

Contract No. W-7405-eng-48

ELECTRON CAPTURE AND THE AUGER EFFECT IN THE HEAVIEST ELEMENTS

Peter Rygaard Gray
(Thesis)

August 1955

Printed for the U. S. Atomic Energy Commission

TABLE OF CONTENTS

	Page
LIST OF TABLES	3
LIST OF ILLUSTRATIONS	5
ABSTRACT	7
I. INTRODUCTION	8
A. The Auger Effect	8
B. Electron Capture	9
II. EXPERIMENTAL METHODS	12
A. Production and Purification of Isotopes	12
B. Instrumental Methods	17
III. EXPERIMENTAL RESULTS	19
A. The Auger Effect	19
1. Tm^{170}-Yb^{170}	19
2. At^{211}-Po^{211}	24
3. Np^{236}-U^{236}	28
B. Decay Schemes	33
1. Np^{236}	33
2. At^{211}	37
3. Po^{207}	43
4. Em^{211}	60
5. At^{209}	79
IV. DISCUSSIONS	81
A. The Auger Effect	81
B. Electron Capture	93
V. ACKNOWLEDGMENTS	105
VI. REFERENCES	106

LIST OF TABLES

		Page
1.	Electron lines from Tm^{170} beta decay	23
2.	Relative intensities of conversion electron lines of 84.4-kev gamma ray in the decay of Tm^{170}	23
3.	Energies and relative intensities of K Auger electrons from At^{211} decay	29
4.	Electron lines of Np^{236}	32
5.	Electromagnetic radiation following the decay of At^{211}	40
6.	Electromagnetic radiations of Po^{207}	45
7.	Low energy internal conversion electrons in the decay of Po^{207}	47
8.	High energy internal conversion electrons in the decay of Po^{207}	48
9.	K/L conversion electron ratios in the decay of Po^{207}	55
10.	Theoretical intensities of gamma rays in the decay of Po^{207}	56
11.	Electromagnetic radiations of Em^{211}	65
12.	Gamma-gamma coincidence studies on Em^{211}	66
13.	Internal conversion electrons of Em^{211} observed on the permanent-magnet spectrographs	68
14.	Internal conversion electrons of Em^{211} observed on the magnetic-lens spectrometer	72
15.	K/L conversion electron ratios in the decay of Em^{211}	73
16.	Comparison of the experimental and theoretical values of the Auger yield of ytterbium, polonium, and uranium	83

Page

17. Recent data on fluorescence yield values 86

18. Experimental ratios of K-LX to K-LL transitions as measured by various observers 90

19. Experimental and theoretical relative intensities of K Auger lines 92

20. Selection rules for beta decay..... 96

21. Log ft values for nuclides whose electron capture decay schemes are known or can be inferred 101

LIST OF ILLUSTRATIONS

		Page
Fig. 1a.	Electron spectrum of Tm^{170}	21
1b.	K Auger electron spectrum of Tm^{170}	22
Fig. 2.	K Auger electron spectrum of At^{211}	26
Fig. 3.	Electron spectrum of Np^{236}	31
Fig. 4.	Decay scheme of Np^{236}	34
Fig. 5.	Spectrum of K x-ray energy region of At^{211}	41
Fig. 6.	Half-life determination of At^{211}	44
Fig. 7.	Gamma spectrum of Po^{207}	46
Fig. 8a.	Electron spectrum of Po^{207}	49
b.		50
c.		51
Fig. 9a.	Radioactive decay of the conversion electrons of	52
b.	Po^{207}	53
Fig. 10.	Decay scheme of Po^{207}	57
Fig. 11a.	Neutron binding energy cycle (general)	59
b.	Neutron binding energy cycle of Po^{207}	59
Fig. 12a.	Gamma spectrum of Em^{211}	62
b.		63
c.		64
Fig. 13.	Gamma rays in coincidence with 675-kev radiation	67
Fig. 14a.	Electron spectrum of Em^{211}	69
b.		70
c.		71
Fig. 15.	Energy levels of At^{211}	76
Fig. 16.	Neutron binding energy cycle of Em^{211}	78
Fig. 17.	General decay scheme of Em^{211}	80
Fig. 18.	Alpha spectrum of At^{209}	82

Page

Fig. 19. Graphical summary of fluorescence yields..... 85

Fig. 20. Variation of $1/W_K$ with $1/Z^4$ in the heavier elements..... 88

Fig. 21. Graphical summary of the ratio of K-LX to K-LL Auger transitions 91

Fig. 22. Log of the partial electron capture half-life versus log of the neutrino energy for allowed electron capture 100

Fig. 23. Log of the partial electron capture half-life versus log of the neutrino energy for forbidden electron capture 104

Electron Capture and the Auger Effect in the Heaviest Elements

Peter Rygaard Gray
Radiation Laboratory and Department of Chemistry
University of California, Berkeley, California

August 1955

ABSTRACT

The Auger effect in the heaviest elements has been investigated. K Auger yields for ytterbium, polonium, and uranium of 0.064 ± 0.01, 0.058 ± 0.005, and 0.033 ± 0.010, respectively, were obtained. The K Auger electrons of ytterbium and polonium were resolved into two groups, K-LL and K-LX, according as two or one L electrons were involved. The ratios of the intensities of the K-LX electrons to the K-LL electrons for ytterbium and polonium were found to be 0.64 ± 0.05 and 0.55 ± 0.03, respectively. A summary of measurements of K fluorescence yields and K Auger electron intensity ratios is given.

The nuclear decay properties of several nuclides in the heaviest elements have been investigated. The electron capture decay of Np^{236}, At^{211}, Po^{207}, and Em^{211} has been studied and decay schemes have been proposed. In addition, the alpha spectrum of At^{209} has been observed.

Log ft values have been calculated for 18 electron-capture nuclides in the heaviest elements whose decay schemes are known or can be inferred from beta decay. These log ft products have been used to classify the electron-capture transitions as to forbiddenness. A logarithmic plot of the electron capture partial half-life versus neutrino energy has been made for both the allowed and forbidden species.

Electron Capture and the Auger Effect in the Heaviest Elements

Peter Rygaard Gray
Radiation Laboratory and Department of Chemistry
University of California, Berkeley, California

August 1955

I. INTRODUCTION

A. The Auger Effect

In the study of the orbital electron capture process in the heaviest elements, it often becomes necessary to know the number of K electron shell vacancies produced by the capture process as well as by internal conversion of gamma radiation. Reorganization in such an ionized atom with a vacancy in the K electron shell can take place in either of two ways.[1] First, a transition may occur during which an electron from a higher energy level fills the vacancy, and the excess energy is emitted as the characteristic electromagnetic radiation (K x-rays) of the element. Secondly, "radiationless" reorganization may take place by the transference of the excess energy to an electron in a higher energy level and the subsequent ejection of this electron from the atom. These ejected electrons are known as K Auger electrons, and the process of their radiationless emission is known as the Auger effect.

If the magnitude of this effect is known, a determination of the number of K shell vacancies can be made by a count of either the K x-radiations or the K Auger electrons. The K Auger coefficient is defined as the number of K Auger electrons emitted per K shell vacancy. A more widely-used term is the K fluorescence yield W_f, defined as the number of the K x-radiations emitted per K shell vacancy. It is obvious that the sum of the K Auger coefficient and the K fluorescence yield is unity.

Recently, a compilation of K fluorescence yields became available[2] which unfortunately contained no information on W_f above polonium ($Z = 84$). Because of the rather extensive research now being conducted on the heaviest elements, data on the Auger effect in the translead region would be highly desirable. This study attempts to remove an inconsistency in the value of W_f for polonium[3] and extend our knowledge of the Auger effect to atomic numbers greater than 84.

B. Electron Capture

Since the characteristic features of positive and negative electron emission and orbital electron capture are so similar, they are all classified as beta decay. Stability considerations for beta decay require only that a parent nuclide be heavier than, that is unstable toward, a neighboring isobar with the resultant transformation of a neutron into a proton or vice versa. There are then three broad types of beta decay:[4]

(1) $n \rightarrow p + e^- + \eta$ (negatron emission).

Negatron emission is observed throughout the periodic system by nuclei with neutron-to-proton ratios greater than those of the beta-stable nuclei of a given element:

(2) $p \rightarrow n + e^+ + \eta$ (positron emission).

Positron emission is observed in elements below mercury ($Z = 80$) by nuclei with neutron-to-proton ratios smaller than those of the beta-stable nuclei of a given element. Recently positron emission was detected for the first time in elements heavier than bismuth when the positron emission/electron capture branching ratio of Np^{234} was observed[5] to be 4.6×10^{-4}.

(3) $p + e^- \rightarrow n + \eta$ (electron capture)

Electron capture is observed throughout the periodic system by nuclei with neutron-to-proton ratios smaller than the beta-stable nuclei of a given element. Electron capture predominates relative to positron emission in the heaviest element region.

The energetic conditions for electron capture require only that the parent atom, Z^A, be heavier than its neighboring isobar, $(Z-1)^A$, by an amount equal to the binding energy of the electron in the particular shell from which capture occurs. When electron capture has taken place, the disintegration energy in excess of the binding energy of the electron in its shell is dissipated as kinetic energy of the emitted neutrino and the recoil nucleus. If, as a result of the electron capture process, the daughter nucleus is left in an excited state, gamma radiation will be emitted. The resultant vacancy in the electron shell is filled by an electron from a higher-energy level, the excess energy being emitted as the characteristic electromagnetic radiations (K, L, etc. x-rays) of the element. Thus, although the electron-capture process is easily detected by observing the characteristic x-rays, no simple method is known for the determination of the decay energy because the emitted particle, a neutrino, has only been observed indirectly, due to its extremely weak interaction with matter.

A few experimental determinations of electron-capture decay energies have been made but almost entirely in the region of the lighter elements. If positron emission competes with electron capture, the electron-capture decay energy can be readily calculated from a knowledge of the maximum energy of the positron and the decay scheme. The continuous gamma

spectrum accompanying electron capture has also proved useful in a few optimum instances[6, 7, 8] for the determination of the electron-capture decay energy. Usually, the neutrino carries off the entire decay energy, but it may also be shared with a photon. The maximum energy of this photon spectrum corresponds to the situation when the entire energy is carried off by the photon: the determination of the endpoint of the photon spectrum is thus an accurate measurement of the decay energy. Another method of measuring electron-capture decay energies is the precise determination of the reaction thresholds such as that of the (p, n) reaction. While the determination of the (p, n) reaction threshold is not applicable in the heaviest elements because the energetic threshold lies below the value for the potential barrier between a proton and the target nucleus, other reaction thresholds such as that of the (α, p3n) reaction may be of value in the heavy-element region for the determination of electron-capture decay energies.

In the heaviest elements, refinements in alpha- and negatron-decay systematics[9, 10, 11] enable calculation of electron-capture total decay energies to be made. However, due to the uncertainties in many of the decay schemes and the difficulty of evaluating the relative effects of K, L, etc., electron capture, only very limited correlations of the electron capture, half-life energy reations, and systematics, have been made. These limited data have been treated by Thompson,[12] Feather,[13] Hoff and Thompson,[14] Major and Biedenharn,[15] and Glass, Thompson, and Seaborg[11] in attempts to obtain fundamental information about the nature of the electron-capture decay process in the heaviest elements. Their results, however, are quite fragmentary and indicate that a more thorough study of the process is necessary before successful theoretical

conclusions can be drawn. This investigation is then a continuation of this program of a detailed study of the orbital-electron-capture process in the heaviest elements, involving especially the study of electron-capture decay schemes.

II. EXPERIMENTAL METHODS

A. Production and Purification of Isotopes

Two milligram and 10 microgram samples of Tm^{169} (greater than 99 percent thulium) in the form of thulium oxide were irradiated with slow neutrons in the Materials Testing Reactor at the Reactor Testing Station, Arco, Idaho, for periods of 24 hours and 10 days, respectively. Tm^{170}, a 129-day negatron emitter was formed by the (n, γ) reaction. The 2 milligram sample was purified by ion-exchange techniques using ammonium lactate as the eluant[16] to separate the thulium from the other rare earths present as less than 1 percent impurity. Approximately 2×10^9 disintegrations per minute of Tm^{170} (less than 10 percent of the 2 milligram sample) was sublimed onto 0.00025-inch thick platinum using a high geometry sublimator[17] for use in the double-focusing beta spectrometer.

Sources for the permanent-magnet beta spectrographs were prepared from the 10 microgram sample of Tm^{170}. Approximately 10^8 disintegrations per minute of Tm^{170} were electrodeposited on 15-mil platinum wires by the electrodeposition process suggested by Harvey[18] and modified by Smith.[19]

At^{209} and At^{211} were prepared by the bombardment of bismuth metal which had been melted onto a 0.010-inch aluminum plate in a layer approximately 0.050-inch thick. These targets were clamped

in a water-cooled target holder and mounted so as to intercept the full deflected helium-ion beam of the 60-inch cyclotron of the Crocker Radiation Laboratory. At^{209} was prepared by an (α, 4n) reaction on the Bi^{209} target using the full-energy beam of helium ions (48 Mev). Smaller amounts of At^{210} and At^{211} were produced also by (α, 3n) and (α, 2n) reactions, respectively. At^{211}, essentially free of other astatine isotopes, was prepared by an (α, 2n) reaction on the Bi^{209} target by attenuating the helium-ion beam to 29 Mev with 0.001-inch platinum foils.[20] In all bombardments, the helium-ion beam was limited to 15 microamperes to prevent loss of astatine due to overheating of the bismuth target.

The requirement that the astatine be present in a narrow line source necessitated modifications of the methods of Barton, et al.[21] which utilize the high volatility of astatine in the zero valence state as compared to bismuth, lead, and polonium. It was found that temperatures as high as 700° C could be used without contaminating the astatine with bismuth, lead, or polonium. A line source was prepared for the double-focusing beta spectrometer by employing a 0.001-inch copper plate with a 3/8 x 1/16-inch slit as a collimating plate over a thin (157 micrograms/cm^2) palladium leaf. In later experiments, silver leaf was substituted for the palladium to utilize the greater affinity of silver for astatine.[22] Sources of At^{211} for the bent-crystal spectrometer were prepared similarly with the exception that the copper collimating plate was removed, the astatine activity being collected on the entire surface of the silver leaf. The silver leaf was then packed in thin (0.015 inch) Pyrex capillaries.

An alternate method was also employed for preparing samples of At^{211} for the bent-crystal spectrometer and permanent-magnet spectrographs and At^{209} for the alpha-particle spectrograph. The bismuth target material was melted in a quartz tube in a vacuum system. A stream of nitrogen (1 to 2 mm pressure) prevented the astatine from condensing on the glass surfaces of the system. The astatine was collected on a liquid nitrogen cooled finger, coated with a thin layer of ice which contained a small amount of perchloric acid. The layer of ice was melted into a small centrifuge cone. Fifteen-mil silver wires, approximately 1 1/16 inch long, were placed in the melt, and the solution was stirred for approximately 1 hour. The astatine deposits on the wire in a manner thought to be analogous to the preparation of I^{131} silver wire sources.[19] These wires were then mounted directly in the bent-crystal spectrometer, permanent-magnet beta spectrographs, and alpha-particle spectrograph.

Np^{236} was produced by a (d, n) reaction by the bombardment of uranium foil containing greater than 99 percent U^{235} with 12.5-Mev deuterons from the 60-inch cyclotron of the Crocker Radiation Laboratory. The activity level of the Np^{235} formed by the (d, 2n) reaction was expected to be low because of its long half-life (410 days). After separation and purification,[23] a source of Np^{236} for the double-focusing beta spectrometer was prepared by the evaporation of a drop of distilled water containing the Np^{236} activity from thin palladium leaf backing.

Em^{211} was prepared by the spallation of thorium foils with 340-Mev protons in the internal beam of the 184-inch cyclotron. Preparation of the Em^{211} sources was not begun until approximately 12 hours after

the end of the irradiation to allow the shorter-lived emanation isotopes to decay. With the exceptions of Em^{211} (16-hour half-life) and Em^{222} (3.8-day half-life), the longest-lived emanation isotope known is Em^{210} (2.7-hour half-life). Em^{222} was not expected to interfere with the Em^{211} measurements since the initial activity level of the Em^{222} at the end of the irradiation is less than 1 percent[24] of the Em^{211}. Em^{211} sources for the permanent-magnet beta spectrographs, the magnetic-lens beta spectrometer, and the pulse analyses of gamma rays and x-rays were prepared by the glow-discharge technique.[24] The Em^{211} activity was deposited on 0.015-inch platinum wires for use in the permanent-magnet beta spectrograph. For the magnetic-lens beta spectrometer and the gamma-ray and x-ray pulse analyses, sources of Em^{211} were deposited on one side of 0.001- and 0.005-inch aluminum plates by suitable masking of the plates.

Po^{207} was prepared by two methods. In the first, it was recovered as the alpha daughter of Em^{211} which exhibits branching decay, 25 percent alpha decay to Po^{207}, and 75 percent electron-capture decay[25] to At^{211}. After separating the Em^{211} prepared by the spallation of thorium with 340-Mev protons, the 5.7-hour Po^{207} activity was allowed to grow for approximately 12 hours. The Po^{207} and At^{211} were then removed from the vacuum system with a few milliliters of concentrated hydrochloric acid. After dilution to 6 N HCl, the Po^{207} and At^{211} were extracted with stirring for five minutes into a mixture containing 20 percent tributyl phosphate and 80 percent dibutyl ether. The organic layer containing the Po^{207} and At^{211} and smaller amounts of lead and bismuth was scrubbed two times with 6 N HCl to remove the lead and bismuth. The Po^{207} and At^{211} were back-extracted out of the organic layer with concentrated nitric acid.

The At^{211} contamination in the Po^{207} was not objectionable because its gamma-ray and conversion-electron spectra have been thoroughly studied.[26, 27] Sources for the permanent-magnet beta spectrographs were prepared by placing 15-mil silver wires, approximately 1 1/16 inch long, in the re-extract and stirring for approximately 1 hour. Polonium and astatine deposit on the wire in a manner which is thought to be analogous to the preparation of I^{131} silver wire sources.[19] Sources for gamma-ray and x-ray spectroscopy were prepared by the evaporation of a drop of the re-extract on platinum plates.

Po^{207}, free of astatine contamination, was prepared by the helium-ion bombardment of lead chloride, enriched in Pb^{206}, in the 60-inch cyclotron of the Crocker Radiation Laboratory. A special target assembly, a pistol-grip target holder which has been discussed elsewhere,[28] was used for the irradiation. The helium-ion beam was attenuated to approximately 40 Mev with a 1-mil platinum foil. The Po^{207} was formed by an (α, 3n) reaction on Pb^{206}. Because of their long half-lives relative to Po^{207}, 2.9-year Po^{208} formed by an (α, 2n) reaction and approximately 100-year Po^{209} formed by an (α, n) reaction were expected to exhibit low activity levels.

Po^{207} was recovered from the lead chloride target by a modification of the method of Treiman, et al.[29] which uses the glass wool adsorption of colloidal polonium hydroxide as a means of separating polonium from lead and bismuth. The lead chloride target was dissolved in hot, weak hydrochloric acid (pH of 4.3) containing the glass wool. After dissolution was complete, the solution and glass wool were heated for 15 minutes. The glass wool was removed and thoroughly washed with hot water. The Po^{207} was removed by leaching with

concentrated hydrochloric acid. After dilution to 6 N HCl, the Po^{207} was further purified by the solvent extraction method described above. The overall chemical yield of Po^{207} was estimated to be approximately 25 percent. Sources for the magnetic-lens beta spectrometer were prepared by the evaporation of a drop of the nitric acid re-extract on 0.025-inch platinum.

B. Instrumental Methods

Various types of beta-ray spectrometers or spectrographs were used to analyze the conversion and Auger electron lines and the beta spectra. A double-focusing, $\pi\sqrt{2}$, magnetic, beta-ray spectrometer,[17,30] was especially useful for the intensity measurements necessary in the study of the Auger effect. A side-window, Geiger-Müller counter with a thin window of vinyl plastic supported on a grid of 0.0005-inch diameter tungsten wire was used as a detector. The counter was filled to a regulated pressure of 15 cm total counter gas pressure with a mixture of argon (83 percent) and ethylene (17 percent). The transmission factor for 20-kev electrons through these thin windows was about 100 percent. High resolution (approximately 0.7 percent) allowed intensity measurements of conversion and Auger electron lines to be made. Because of the lack of a precise field-measuring device, absolute energy determinations were not good with this instrument. However, energy differences between electron lines were considered good. Nuclides which have been useful in calibrating the instrument are Cs^{137}, I^{131}, Ta^{182}, Ir^{192}, and Am^{241}.

Precise energy determinations were made on the permanent-magnet 180^{o} spectrographs.[19] The very high resolution (0.15 percent on the

50-gauss spectrograph and 0.2 percent on the 100-gauss spectrograph) allowed the separation of individual Auger electron lines as well as conversion electron lines of gamma rays with very similar energies. Since the electron lines are well resolved, relative intensities of the electron lines can be obtained although perhaps not quite as accurately as with the double-focusing beta spectrometer. The two permanent-magnet spectrographs allowed the study of electron lines with energies up to approximately 275 kev.

A third type of beta-ray spectrometer used extensively was a magnetic lens-type spectrometer with somewhat lower resolution (5 percent) but considerably higher transmission. This allowed the study of nuclides whose activity level was too low for use in the double-focusing beta spectrometer. The use of an anthracene crystal detector sealed to a photomultiplier tube limited the instrument to electrons with energies greater than approximately 150 kev.

The K x-rays and gamma spectra of At^{211} were studied with a 10-inch, bent-crystal spectrometer of the Cauchois type. This instrument has been described by Barton, et al.[31] and further modifed by Browne[32] and Jaffe.[23]

Gamma-ray and x-ray spectroscopy was accomplished using a sodium-iodide (thallium activated) crystal detector, 1 x 1 1/2 inches in diameter, in optical contact with a Dumont-6292 photomultipler tube. The fluorescent radiation from the crystal detector was converted to electronic pulses in the photomultiplier tube. After amplification, the pulses were sorted according to energy in a 50-channel differential pulse analyzer.[33] Gain and bias controls permitted the study of any predetermined energy interval. Gamma-gamma coincidence studies

incorporated the above equipment with a second, single-channel, pulse-height analyzer as described by Stephens.[34]

L x-rays and gamma rays in the 10 to 60 kev range were measured using a xenon-filled (90 percent xenon and 10 percent methane at 1 atmosphere) proportional counter connected to the 50-channel pulse analyzer.

Alpha-emitting nuclides were studied in a 48-channel, differential, alpha-particle pulse analyzer[35] when discrimination of energies was desired. An alpha-particle spectrograph[36] was used to determine the precise energy of the alpha particles of At^{209}.

Radioactive decay of alpha-emitting nuclides was followed with an argon-filled ionization chamber connected to a standard amplifier scalar. Beta-decaying samples were measured on a windowless proportional counter with a continuous methane flow. This instrument was especially useful for electron-capture isotopes because of a favorable counting efficiency for low-energy electrons.

III. EXPERIMENTAL RESULTS

A. The Auger Effect

1. Tm^{170} - Yb^{170}

The summary of K fluorescence yields published recently by Broyles, et al.[2] contains no information on the elements between praseodymium (Z = 59) and platinum (Z = 78). Data on the Auger effect in this region would seemingly be quite useful as an aid to the extrapolation of the Auger coefficient to the heaviest elements. Tm^{170} (Z = 70) appeared to be an ideal isotope to study in this region.

Tm^{170} decays to Yb^{170} by the emission of two beta groups. A 968-kev (maximum energy) beta group in 76 percent abundance decays to

the ground state of Yb^{170}, and a 884-kev (maximum energy) beta group (24 percent) decays to an excited level in Yb^{170} 84.4 kev above the ground state. This excited state decays to the ground state by the emission of electric quadrupole radiation of 84.4 kev.[37] Although Tm^{170} is a shielded nucleus and decay by electron capture must be considered, an upper limit of 0.2 percent for this mode of decay has been set by Jaffe.[23] Therefore, the only K electron shell vacancies produced during the decay of Tm^{170} arise from the K shell internal conversion of the 84.4-kev gamma ray.

Since the K Auger coefficient is the ratio of the number of K Auger electrons emitted to the total number of K electron shell vacancies, the K Auger coefficient of ytterbium can be readily determined if the intensities of the K Auger electrons and the K shell internal conversion electrons of the 84.4-kev gamma ray are known. In order to make such a determination, a sample containing approximately 2×10^9 disintegrations per minute of Tm^{170} was sublimed onto 0.00025-inch platinum as a source for the double-focusing beta spectrometer.

The K Auger and internal conversion electron spectrum obtained is shown in Fig. 1a. The K Auger electron spectrum is shown in greater detail in Fig. 1b. While the K Auger electrons are present in low intensity, two groups corresponding to the K-LL and K-LX (where X refers to the summation of the M, N, etc., atomic orbitals) groups of lines are clearly resolved.

Relative intensities of the electron lines are listed in Table I.

The K Auger coefficient of ytterbium was found to be 0.064 ± 0.01 and the ratio of the groups of K Auger lines to be K-LL:K-LX = $1.00:0.64 \pm 0.05$. The probable errors given were obtained from a consideration of the statistical errors of the individual points.

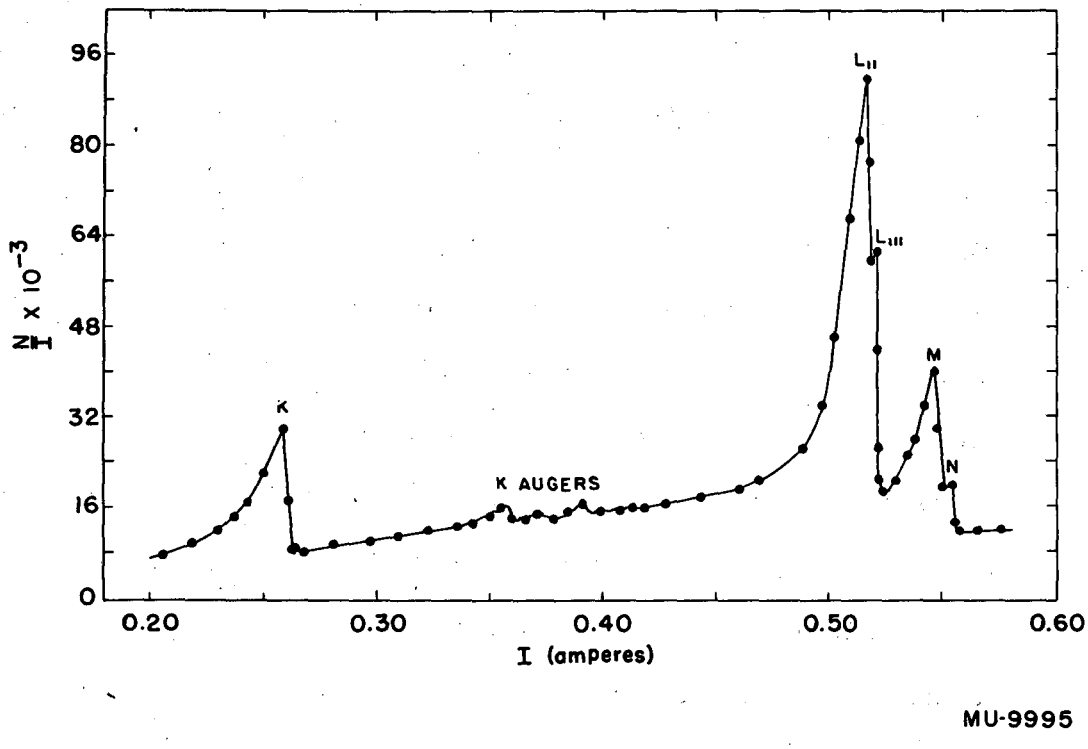


Fig. 1a. Electron spectrum of Tm^{170}.

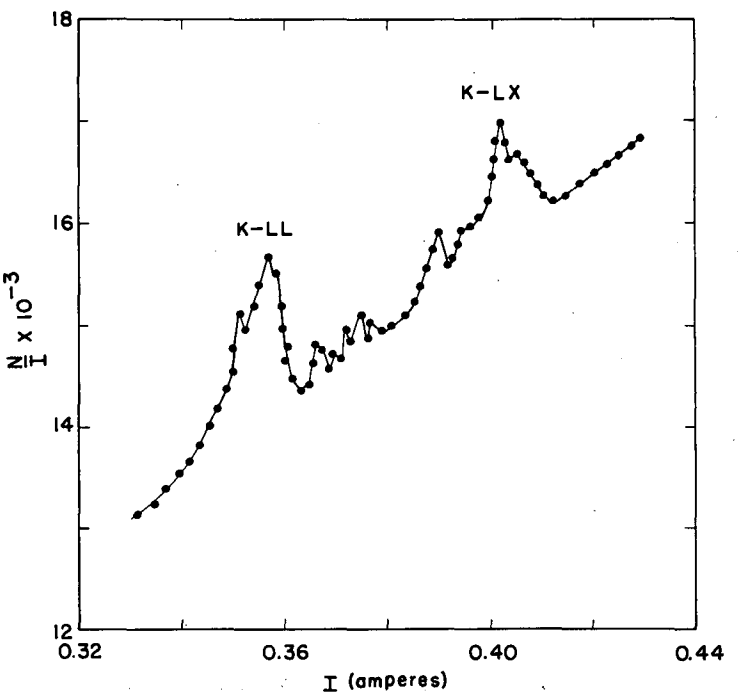


Fig. 1b. K Auger electron spectrum of Tm^{170}.

Table I

Electron Lines from Tm^{170} Beta Decay

Gamma energy (kev)	Electron energy (kev)	Conversion shell	Intensity (arbitrary units)
84.4	23.0	YbK	100
	74.8	YbL	314
	82.4	YbM	72
	94.0	YbN	9.6
K x-rays	40.3 - 43.5	K-LL	3.9
	48.6 - 51.8	K-LX	2.5

Table II compares the relative intensities of the internal conversion electron lines of the 84.4-kev gamma ray with those found by Graham, et al.[37]

Table II

Relative Intensities of Conversion Electron Lines of 84.4-kev Gamma Ray in the Decay of Tm^{170}

Ratio	Graham, et al.[37]	This work
K/L	0.36 ± 0.04	0.32 ± 0.03
K/L+M	0.28 ± 0.03	0.26 ± 0.03
L/M	3.6 ± 0.05	4.3 ± 0.05

Graham, et al.[37] did not resolve the N conversion electrons from the M conversion electrons, and therefore, their values for the ratios containing M should read (M+N).

2. At^{211} - Po^{211}

At^{211} was first made by Corson, et al.[40] in bombardments of bismuth targets with 32-Mev helium ions. They suggested that At^{211} (7.3-hour half-life) showed branching decay, 60 percent electron capture to Po^{211}, and 40 percent alpha emission to Bi^{207}. The branching decay has subsequently been measured to be 59.1 percent electron capture and 40.9 percent alpha emission.[41] Po^{211} decays by alpha emission with a half-life of 0.52 second[41] and is, therefore, in equilibrium with the At^{211}. The Bi^{207} daughter has a half-life which is long enough (8.0 years)[43] so that it may be neglected when studying At^{211}. A careful study has been made by Hoff[26] and Mihelich, et al.[27] of the At^{211} electron-capture decay. No gamma radiation was found, with the possible exception of a 671 ± 5-kev gamma ray in very low abundance (0.37 percent of the astatine electron-capture decay). Although the assignment of this gamma ray to At^{211} is doubtful, its intensity is so low that its contribution to the Auger effect is negligible.

Germain[3] has studied the Auger effect in At^{211} by impregnating photographic emulsions with At^{211} and observing the alpha and Auger electron tracks. His calculated value of 0.106 for the Auger coefficient of polonium appears to be large when compared with other values in the Z = 78 to 83 region.[2, 44]

The Auger effect of astatine can also be studied with the double-focusing beta spectrometer. Since every At^{211} electron capture is followed by an alpha emission from Po^{211}, the number of K shell vacancies can be calculated by a determination of the absolute alpha disintegration rate. If the transmission of the spectrometer is known, the number of K Auger electrons and subsequently the Auger

coefficient of polonium can be calculated by an integration of the K Auger electron spectrum.

The transmission of the double-focusing beta spectrometer was determined using a Th^{228} source. Th^{228} decays to Ra^{224} by the emission of two alpha groups. A 5.423-Mev alpha group in 72 percent abundance decays to the ground state of Ra^{224}, and a 5.338-Mev alpha group (28 percent abundance) decays to an excited level 84.3 kev above the ground state[45] of Ra^{224}. Since the total conversion coefficient (16.5) of the 84.3-kev gamma ray is well known, the transmission of the double-focusing beta spectrometer can be calculated by an integration of the conversion electron spectrum of the 84.3-kev gamma ray.

A sample containing 4.2×10^8 alpha disintegrations per minute of Th^{228} was sublimed onto palladium leaf in a line source, 3/4 x 1/16 inch. The number of electrons in the L, M, and N conversion electron lines of the 84.3-kev gamma ray, obtained by an integration of their spectra, was 2.24×10^4 electrons. Combining this with the total number of electrons expected from the internal conversion of the gamma ray in the sample containing 4.2×10^8 disintegrations per minute of Th^{228} gives a transmission of 0.022 percent for the spectrometer.

Two separate and identical studies of the Auger effect in astatine were made using the double-focusing beta spectrometer. In the first study, a sample containing 7.2×10^8 disintegrations of At^{211} was sublimed onto palladium leaf in a 3/8 x 1/16 inch line source, as a source for the spectrometer. The K Auger electron spectrum is shown in Fig. 2. While the resolution of the instrument does not allow the complete separation of the individual Auger lines, two

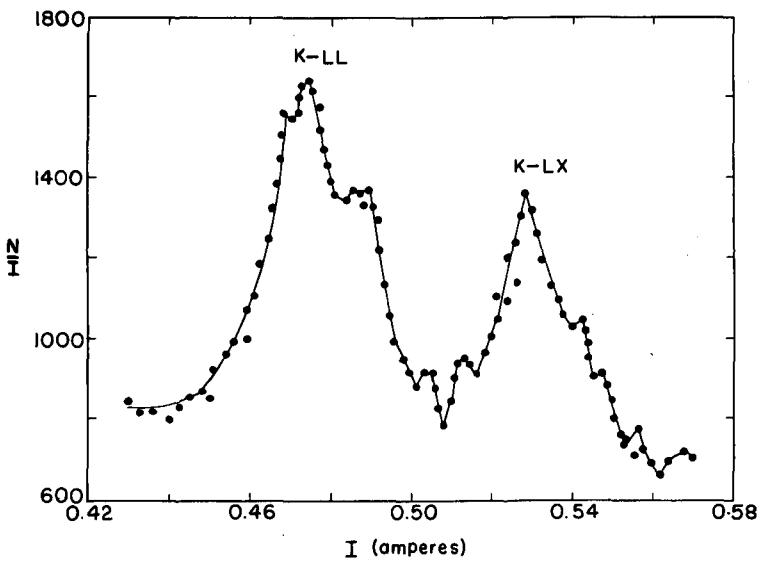


Fig. 2. K Auger electron spectrum of At^{211}.

distinct electron groups are clearly resolved. The first group of electrons, at an energy of 59 to 65 kev, was identified as the K-LL Auger electrons. The second group of electrons at an energy of 72 to 76 kev was identified as the K-LX electrons. The ratio of the two groups was found to be K-LL:K-LX = 1.00:0.55 ± 0.03. The number of electrons in the K Auger line spectrum was 4,250. After correcting for the transmission (0.022 percent) and the branching decay of At^{211} (59.1 percent electron capture), the Auger coefficient of polonium was calculated to be 0.049 ± 0.005. However, this value is calculated on the assumption of pure K electron capture and must therefore be corrected for L electron capture. Rose and Jackson[46] have calculated that for an element in this region of the periodic table the ratio of L electron capture to K electron capture is 0.15. Hoff,[26] using Germain's value of 0.106 for the Auger coefficient of polonium, experimentally determined the K to L electron capture ratio as approximately seven. Correcting this value using an Auger coefficient of 0.05, the experimental K to L electron capture ratio is six. After making this correction for L electron capture in At^{211}, a value of 0.058 ± 0.005 as the Auger coefficient of polonium is obtained.

In the second determination of the Auger coefficient, At^{211} was sublimed onto palladium leaf to give a source, 3/8 x 1/16 inch, containing 2.5×10^8 disintegrations per minute. The K Auger electron spectrum obtained using the double-focusing beta spectrometer contained 1,425 electrons. After correcting for the transmission, the branching ratio of At^{211}, and the L electron capture, a value of 0.056 ± 0.008 is obtained for the K Auger coefficient of polonium which is in good agreement with the previous value. The ratio of the K

Auger electron groups was K-LL:K-LX = 1.00:0.61 ± 0.08.

These values of the Auger coefficient of polonium are upper limits. Since the physical dimensions of the Th^{228} source from which the transmission was obtained was approximately twice the length of the At^{211} sources, this would give a lower limit to the transmission and hence an upper limit to the Auger coefficient.

This result of 0.058 for the Auger coefficient of polonium is in better agreement with the values expected in this region. A possible explanation of Germain's high value is discussed in Section III, B-2.

Precise energies of the K Auger electrons from At^{211} were obtained using the 50-gauss permanent-magnet spectrograph. Table III lists the K Auger electrons observed with their experimental energies. Energies calculated with the Bergström-Hill formula[38] using the critical x-ray absorption energies from Hill, et al.[39] are included for comparison. Experimental relative intensities of the K-LL electrons are included. Intensities of the K-LX electrons were too weak for measurement.

3. Np^{236} - U^{236}

Since no experimental results are available on the Auger effect in the elements above polonium (Z = 84), it would be of interest to measure the Auger coefficient of some nuclide in this region. Np^{236} had been studied previously by Orth and O'Kelley[47] who reported an electron capture to negatron emission ratio of two. Two negatron groups of maximum energy, 0.51 and 0.36 Mev, respectively, were detected as were x-rays and a gamma ray of 150 kev which was reported to be approximately 100 percent internally converted. No

Table III

Energies and Relative Intensities of K Auger Electrons from At^{211} Decay

K auger electron	Energy experimental (kev)	Energy Bergström-Hill[38] (kev)	Relative intensity (arbitrary units)
$K\text{-}L_IL_I$	59.07	58.97	6.9
$K\text{-}L_{II}L_I$	59.75	59.67	10.0
$K\text{-}L_{III}L_I$	62.19	62.10	4.3
$K\text{-}L_{II}L_{III}$	62.83	62.80	9.4
$K\text{-}L_{III}L_{III}$	65.33	65.22	4.8
$K\text{-}L_{II}L_{II}$	--	60.37	<1
$K\text{-}L_IM_I$	72.01	71.98	--
$K\text{-}L_IM_{II}$	72.32	72.29	--
$K\text{-}L_IM_{III}$	72.91	72.86	--
$K\text{-}L_{II}M_{II}$		72.99	--
$K\text{-}L_IM_V$	73.62	73.47	--
$K\text{-}L_{II}M_{III}$		73.56	--
$K\text{-}L_{III}M_{II}$	75.46	75.41	--
$K\text{-}L_{III}M_{III}$	76.04	75.98	--

other gamma radiations were observed. This isotope, then, appeared to be ideal for studying the Auger effect since the number of K vacancies could be determined through a knowledge of the decay scheme, the transmission of the double-focusing beta spectrometer, and integrations of the K internal conversion electron spectrum of the 150-kev gamma ray and the negatron spectrum. The number of K Auger electrons and, hence, the Auger coefficient could then be determined from an integration of the K Auger electron spectrum.

A source of Np^{236} was studied on the double-focusing beta spectrometer. An electron spectrum was observed which was similar to that obtained in the previous work.[47] However, certain lines in the spectrum showed greater complexity than before. Coupled with recent gamma-ray and x-ray spectroscopy studies,[23] a reinterpretation of the data became necessary, and a new decay scheme was proposed.

The electron lines designated as L Auger electrons by Orth and O'Kelley[47] were resolved into four lines which were interpreted as the L_{II} and L_{III} internal conversion electrons of gamma rays with energies 43.5 ± 1 and 44.2 ± 1 kev. A line previously reported as the K conversion line of a 150-kev gamma ray may also be interpreted as the unresolved M conversion electrons of the 43.5- and 44.2-kev gamma rays. Unresolved N conversion electrons were also observed as were K Auger electrons.

The electron spectrum obtained is shown in Fig. 3, and the electron data are summarized in Table IV.

The K electron capture/negatron emission branching ratio in the Np^{236} decay was determined to be 43 ± 5 percent/57 ± 5 percent from the alpha-particle disintegration rate (Pu^{236}) and the absolute

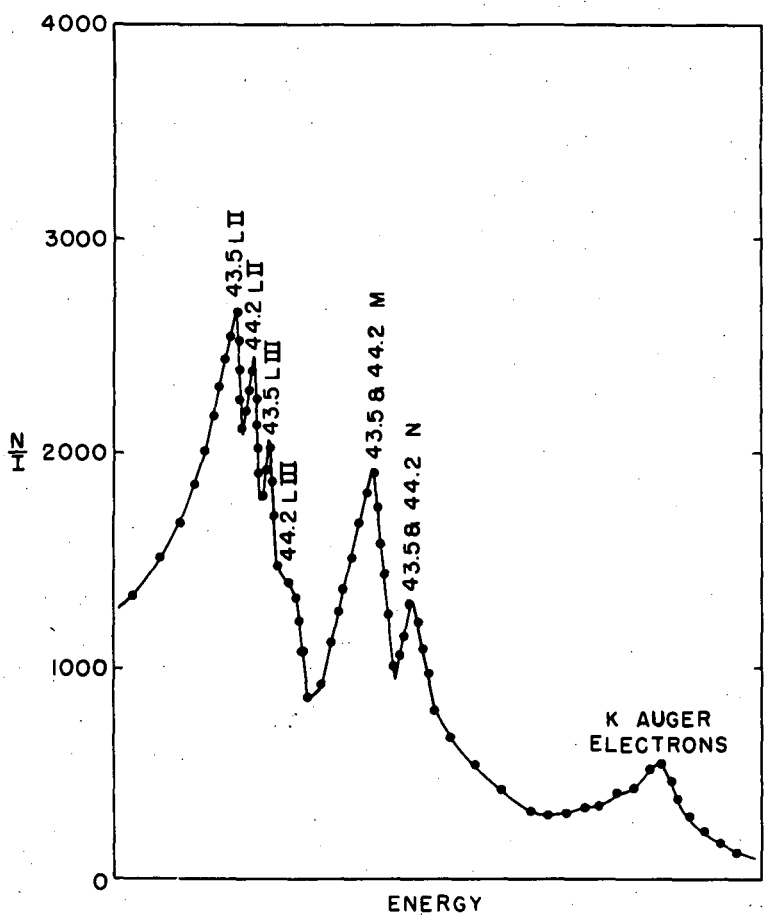


Fig. 3. Electron spectrum of Np^{236}.

Table IV

Electron Lines of Np^{236}

Gamma energy (kev)	Electron energy (kev)		Conversion shell	Intensity (arbitrary units)
43.5 ± 1	21.1		PuL_{II}	48
	25.4		PuL_{III}	
44.2 ± 1	23.2		UL_{II}	
	27.0		UL_{III}	
44 ± 2	37.9		PuΣM	18
		and	UΣM	
43 ± 1	41.7		PuΣN	3
		and	UΣN	
K x-rays	88 ± 5		UΣL	5*
		and	UΣM	
	(K Auger electrons)			
--	500 ± 30		--	200
	(β^- maximum)			

*Incorrectly reported as 10 by Passell.[17]

abundance of the K x-rays at the beginning of the experiment. The K x-ray intensity was corrected for the presence of Np^{234} and an estimated fluorescence yield of 97 percent.

Through an analysis of the L x-rays, K x-rays, and relative intensities of the L internal conversion electrons of the 43.5- and 44.2-kev gamma rays, it appears safe to conclude that approximately

80 percent of both the negatron emission and K electron capture decay of Np^{236} lead directly to the ground states of Pu^{236} and U^{236}, respectively. The decay scheme is shown in Fig. 4, and will be more fully discussed in Section III, B-1.

A value of the K Auger coefficient of uranium can now be obtained through a knowledge of the decay scheme and the relative intensities of the electrons. A knowledge of the transmission of the spectrometer is not necessary in this calculation. The relative intensity of the internal conversion electrons from both the 43.5- and 44.2-kev gamma rays is 69. Since each excited state in U^{236} and Pu^{236} is approximately evenly populated (20 percent) and the K electron capture branching is 43 percent, we have a relative intensity of 30 for the 43.5-kev gamma ray resulting from the electron-capture decay of Np^{236}. However, since these L internal conversion electrons occur in only 20 percent of the transitions, this corresponds to a total of 150 transitions. Assuming K electron capture only, an assumption upon which the branching ratio was determined, this corresponds to 150 K shell vacancies. It will be shown in Section III, B-1, that the K/L electron capture ratio is large.

Inasmuch as there are 5 K Auger electrons observed relative to the 150 K shell vacancies, the K Auger coefficient of uranium is 0.033 ± 0.010. The limit of error results from the uncertainty in the intensities of the electrons and in the K/L electron capture ratio.

B. Decay Schemes

1. Np^{236}

Np^{236} was first produced by James, et al.[48] from bombardments of uranium with deuterons. The only previous study of the decay

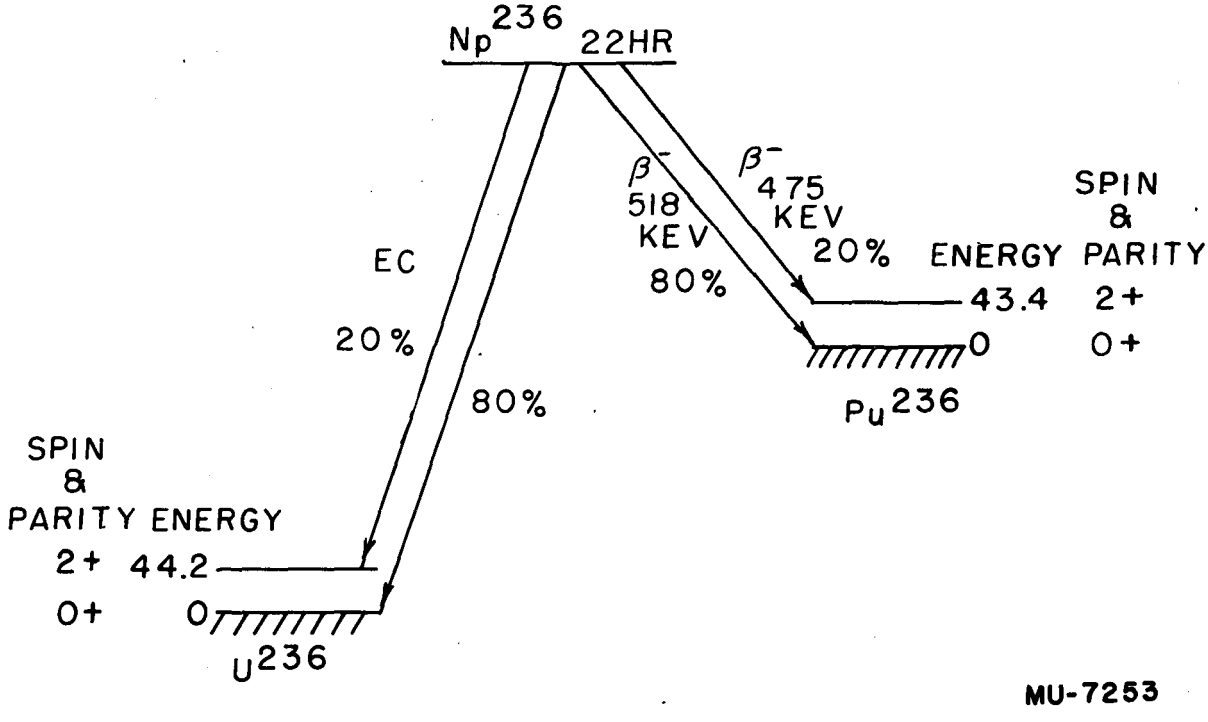


Fig. 4. Decay scheme of Np^{236}.

scheme of Np^{236} was by Orth and O'Kelley[47] who found evidence for electron capture from Auger electron intensities and x-ray abundances. A two-component negatron spectrum with maximum energies 0.51 and 0.36 Mev, respectively, was detected, as were prominent K internal conversion electrons and very weak indications of the L conversion electrons from a 150-kev gamma ray. They concluded that the gamma ray followed the soft negatron component, and as no other gamma radiation was detected, the electron capture populated the ground state of the U^{236} daughter. The electron capture/negatron emission branching ratio was estimated as two. The L electron capture/K electron capture ratio was also estimated as two.

In the present study, Np^{236} was investigated on the double-focusing beta spectrometer. An electron spectrum was obtained which was very similar to that of the previous workers. However, some of the electron lines showed greater complexity than before. The electrons designated as L Auger electrons by Orth and O'Kelley were resolved into the L_{II} and L_{III} conversion electrons of two gamma rays of 43.5 ± 1 kev and 44.2 ± 1 kev, respectively. A line previously reported as the K conversion electrons of a 150-kev gamma ray may also be interpreted as the unresolved M conversion electrons of the 43.5- and 44.2-kev gamma rays. Unresolved N conversion electrons were also observed, as were K Auger electrons. The electron spectrum is shown in Fig. 3. The electron intensity data are summarized in Table IV in the previous section.

The assignment of the 43.5-kev gamma ray to Pu^{236} and the 44.2-kev gamma ray to U^{236} is quite arbitrary. The latter is in good agreement with the energy of the 44-kev ray determined[49] for the first

excited state of U^{236} from the alpha particle fine structure of Pu^{240}.

Because the intensity of the negatron spectrum observed on the double-focusing spectrometer was too low for a Fermi analysis, advantage was taken of the higher transmission of the magnetic-lens spectrometer to obtain these data. The Fermi-Kurie plot exhibited a marked concavity toward the abscissa which is indicative of a forbidden transition. The maximum energy obtained was 518 ± 10 kev.[50]

X-ray and gamma-ray spectroscopy revealed no evidence of a 150-kev gamma ray in a thorough examination of the 0- to 200-kev energy region.[23]

The K electron capture/negatron emission ratio was determined by observing the alpha growth of the Pu^{236} daughter. Alpha pulse analysis indicated that only the 5.75-Mev alpha particles of Pu^{236} were present. The alpha particle disintegration rate after the 22-hour Np^{236} had completely decayed, coupled with the absolute abundance of the K x-rays at the beginning of the experiment, indicated the K electron capture/negatron emission branching ratio of Np^{236} as 43 ± 5 percent/57 ± 5 percent. The K x-ray abundance was corrected for the presence of Np^{234} in the sample and a fluorescence yield of 0.97.

X-ray spectroscopy[23] indicated that the intensity of the L x-rays was 0.6 relative to the K x-rays. Making corrections for (1) a mean L x-ray fluorescence yield of[51] 0.5, (2) a K x-ray fluorescence yield of 0.97, (3) 72 percent of the K shell vacancies being filled by L shell electrons,[52] and (4) 43 percent of the disintegrations being due to K electron capture, there are a maximum of 0.48 L shell vacancies from internal conversion per K electron capture decay or 0.21 vacancies per disintegration.

From the electron intensities, the abundance of conversion electrons is about 35 percent of the negatron spectrum. Since 57 percent of the disintegrations take place by negatron emission, there are 20 conversion electrons per 100 disintegrations. Thus, within the limits of error of the intensity measurements, all of the L shell vacancies can be accounted for by the L shell internal conversion of the 43.5- and 44.2-kev gamma rays. However, since the limits of error are such that five to ten L shell vacancies per 100 disintegrations could be arising from L electron capture, it appears safe to conclude that the lower limit for the K/L capture ratio is around four.

Since the intensities of the L electrons from the conversion of the 43.5- and 44.2-kev gamma rays are approximately equal, an upper limit of about ten events per 100 disintegrations populate each of the first excited states of Pu^{236} and U^{236}.

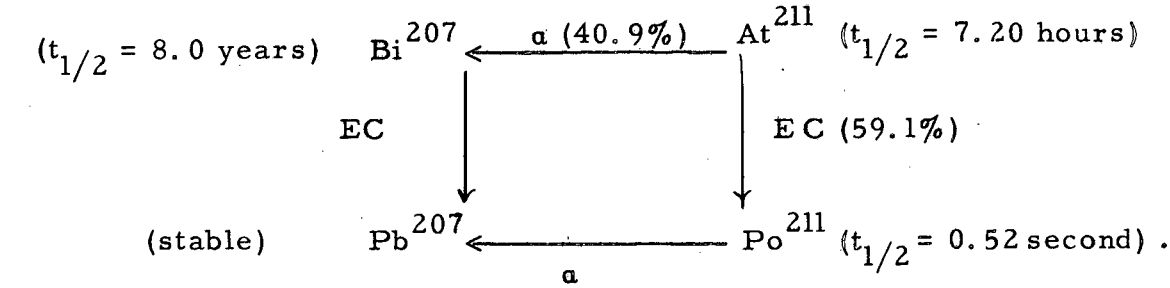
A decay scheme, consistent with the available data, is given in Fig. 4.

The equal intensities of the L_{II} and L_{III} conversion electrons suggest that both gamma rays are E2 transitions. This is consistent with the usual assignment in this region for even-even nuclides of zero spin and even parity for the ground state and spin 2 with even parity for the first excited state.

2. At^{211}

At^{211}, produced by Corson, et al.[40] in bombardments of bismuth with 32-Mev helium ions, was the first isotope of astatine to be identified. It was suggested that the 7.5-hour At^{211} decays 40 percent by emission of a 5.89-Mev alpha particle to Bi^{207} and 60 percent by

electron capture to Po^{211} (AcC'). The Po^{211}, in turn, decays with a very short half-life to stable Pb^{207} by the emission of a 7.43-Mev alpha particle. Further studies by Corson, et al.,[53] using critical absorption methods showed that the electromagnetic radiations observed at 90 kev were polonium K x-rays. The branching ratio of At^{211} has subsequently been measured to be 40.9 percent alpha emission and 59.1 percent electron capture.[41] Po^{211}, the electron capture daughter, has a half-life of 0.52 second,[42] and is, therefore, in equilibrium with the At^{211} after a few seconds. The alpha emission daughter, Bi^{207}, has a half-life (8.0 years)[43] that is long enough so the decay of Bi^{207} may be ignored when studying At^{211}. The decay of At^{211} may be shown diagrammatically as:



Hoff[26] and Mihelich, et al.[27] have recently studied the decay of At^{211}. Hoff was able to set an upper limit of 0.5 percent of the total disintegrations for the total abundance of any electromagnetic radiation other than x-rays, with the exception of radiations with energies nearly identical to those of the polonium x-rays. Mihelich, et al.[27] reported no electromagnetic radiations with the possible exception of a weak (0.37 percent of the total At^{211} disintegrations) gamma ray of 671 kev which was not in prompt coincidence with either alpha particles or K x-rays.

Due to the abnormally high value of the Auger coefficient of polonium determined by Germain[3] as the results of a study of At^{211}, a reinvestigation of this nuclide appeared to be warranted. Germain studied the Auger effect in astatine using a photographic emulsion technique. The emulsion was impregnated with At^{211} and after developing, the number of Po^{211} alpha tracks which had an Auger electron at one end of the track was determined. It was observed in selecting random fields of view that out of a total of 1849 Po^{211} tracks examined, 171 were found to have Auger tracks. After correcting for L electron capture in At^{211} a value of 0.106 was obtained for the Auger coefficient of polonium. This value when compared with the expected value for polonium[2] (approximately 0.05) is about two times too large.

If a gamma ray, of comparable energy to the K x-ray group, were present in approximately 5 percent of the disintegrations of At^{211}, the L internal conversion electrons of this gamma ray would be indistinguishable from the K Auger electron tracks in the photographic emulsions. Because of the low resolution (7 to 10 percent) of the sodium iodide (thallium activated) scintillation crystals used in the gamma and x-ray spectroscopy of At^{211}, a gamma ray of energy 60 to 100 kev in low abundance would probably not be resolved from the abundant K x-rays (80 to 93 kev). In this study advantage was taken of the high resolution of the 10-inch bent-crystal spectrometer to examine the K x-ray region more closely.

A sample containing greater than 10^9 disintegrations per minute of At^{211} was sublimed onto very thin silver leaf, packed into a 15-mm glass capillary, and mounted on the spectrometer. One line was observed which can be ascribed to a gamma ray of 62.35 ± 0.5 kev.

The gamma ray is shown with the K x-ray spectrum in Fig. 5. The four K x-rays observed and their energies and relative intensities are listed in Table V, together with the gamma ray. The relative intensities have been corrected for self absorption in the sample, reflectivity of the crystal, and absorbers in the path between the sample and the detector. Insufficient activity prevented a study of the L x-ray energy region (10 to 25 kev).

Table V

Electromagnetic Radiation Following the Decay of At^{211}

Line	Transition	Energy observed (kev)	Energy accepted (kev)	Corrected relative intensity (arbitrary units)
Po $K\alpha_2$	$K\text{-}L_{II}$	76.89 ± 0.14	76.93	55
Po $K\alpha_1$	$K\text{-}L_{III}$	79.32 ± 0.10	79.35	100
Po $K\beta_1\beta_3$	$K\text{-}M_{II}M_{III}$	89.67 ± 0.17	89.32 - 89.87	26
Po $K\beta_2$	$K\text{-}N_{II}N_{III}$	92.32 ± 0.20	92.31 - 92.45	5.4
Γ		62.35 ± 0.20	--	8.2

At^{211} was also studied on the permanent-magnet beta spectrographs. Besides the K Auger electrons, a 46.0 ± 0.3-kev electron line was observed. On subsequent investigations on the same instrument, however, this 46-kev electron line was either not observed or was observed in varying intensities relative to the K Auger electrons. The 46-kev electrons are probably L shell internal conversion electrons from the 62.3-kev gamma ray observed on the bent-crystal spectrometer. The

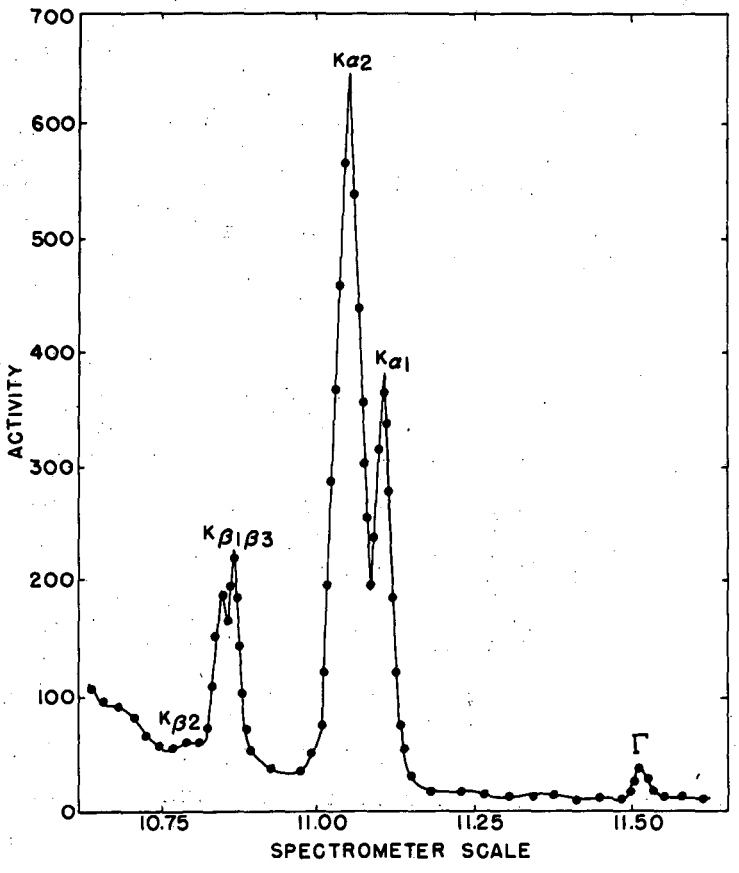


Fig. 5. Spectrum of K x-ray energy region of At^{211}.

possibility that they are K shell internal conversion electrons of a higher energy gamma ray cannot be discounted, however, although no electromagnetic radiation in the energy region between the K x-rays and 150 kev has been observed.

While the varying relative intensity of these electrons is very puzzling, it is believed that they are not due to impurities in the sample since weak 46-kev electrons have been observed in the electron spectrum of Em^{211} which decays to At^{211} by electron capture. (see Section III-B4). A 46-kev electron line, ascribed to the N shell conversion electrons of the rather prominent 47-kev gamma ray in the decay of At^{210} to Po^{210} have been observed by Mihelich, et al.[27] The electrons seen in the At^{211} decay are definitely not due to At^{210} contamination. The ratio of At^{210} to At^{211} produced in a bombardment can be calculated by determining the intensity of the Po^{210} (138-day alpha emitter) after all the At^{211} (7.2 hour) and At^{210} (8.3 hour) have decayed. In the experiments above, the At^{210}/At^{211} ratio has been measured to be less than 10^{-6}.

As only one electron line was observed, it is suggested that the gamma ray is internally converted in the L_I electron shell. The L_I shell electron binding energy of bismuth (16.4 kev) is in agreement with the energies of the electrons and gamma ray observed. This would indicate that the 62.3-kev gamma ray follows the alpha branching of At^{211} to Bi^{207}. However, no complex structure in the alpha branching decay of At^{211} has been observed.[26]

While assignments of the 46.0-kev electrons and the 62.3-kev gamma ray cannot be made, it is possible that these electrons were

observed by Germain,[3] and misinterpreted as K Auger electrons, giving an abnormally high value to the K Auger coefficient.

The half-life of At^{211} has also been redetermined. Corson, et al.[40] and Kelly and Segrè[20] have reported the half-life of At^{211} to be 7.5 hours. Hall and Templeton[54] have reported 7.3 hours for the half-life and Neumann and Perlman[41] report 7.2 hours. Especially purified bismuth was bombarded with 29-Mev helium ions in the 60-inch cyclotron of the Crocker Radiation Laboratory. The radioactive alpha decay of an At^{211} sample mounted on silver to minimize loss of astatine by evaporation was followed for 12 half-lives in an argon-filled ionization chamber (52 percent counting efficiency). As shown in Fig. 6 the radioactive decay curve of At^{211} is straight over the 12 half-lives. This experimentally determined half-life of At^{211} is 7.20 ± 0.05 hours.

3. Po^{207}

Po^{207} was first produced by Templeton, et al.[55] in bombardments of lead with 40-Mev helium ions. Electromagnetic radiation, whose energy was determined by aluminum absorption to be 1.3 Mev, was observed to decay with a half-life of 5.7 ± 0.1 hours. Weak alpha activity was also observed. The alpha particle emission/electron capture branching ratio was estimated to be approximately 10^{-4}. The alpha particle energy has subsequently been measured to be 5.10 ± 0.02 Mev.[56]

In the present study, Po^{207} has been produced as the alpha emission daughter of Em^{211} and also by bombardment of $PbCl_2$, enriched in Pb^{206}, by 40-Mev helium ions. The electromagnetic radiations of this isotope have been studied on the sodium iodide (thallium activated)

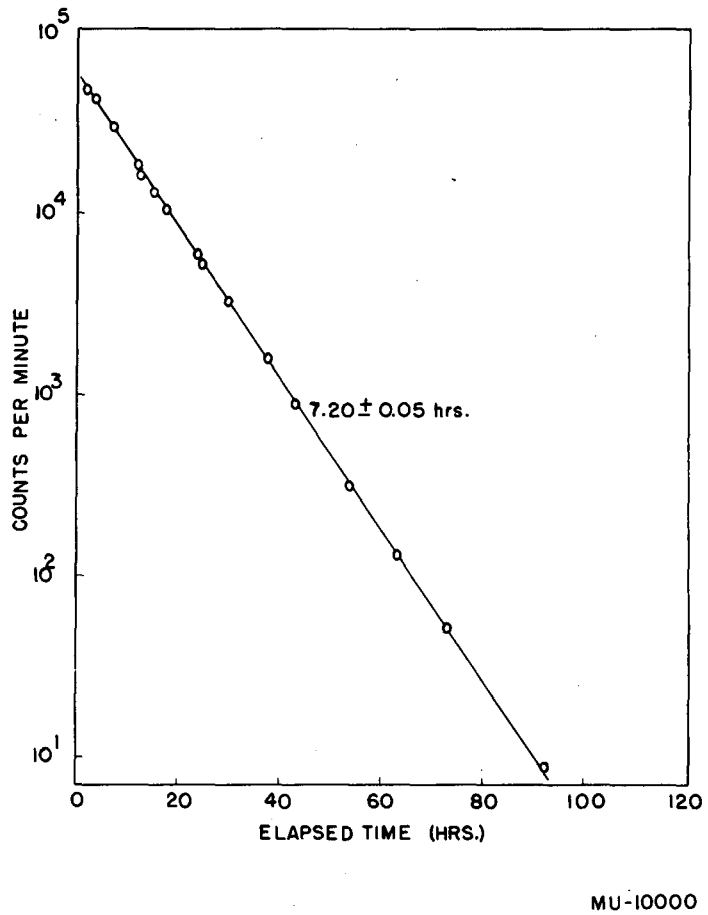


Fig. 6. Half-life determination of At^{211}.

crystal spectrometer. The gamma-ray spectrum (above 400 kev) is shown in Fig. 7. The energies of the gamma rays and their relative intensities are listed in Table VI. The lower energy electromagnetic radiation is expected to be in low intensity because of internal conversion of the gamma rays. The Compton background from the higher energy gamma rays and the intensity of the K x-rays makes the resolution of these lower energy gamma rays difficult.

Table VI

Electromagnetic Radiations of Po^{207}

Energy (kev)	Relative intensity (arbitrary units)
75 ± 5 (K x-rays	--
410 ± 20	22
500 ± 30	0.6
625 ± 30	0.2
765 ± 20	73
980 ± 20	100
1150 ± 30	<1

Data on the low-energy (20 to 250 kev) internal conversion electrons were obtained on the permanent magnet spectrographs. The higher energy conversion electrons (above 150 kev) were observed on the magnetic-lens spectrometer. The electrons observed on the permanent-magnet spectrographs are listed in Table VII together with their relative intensities.

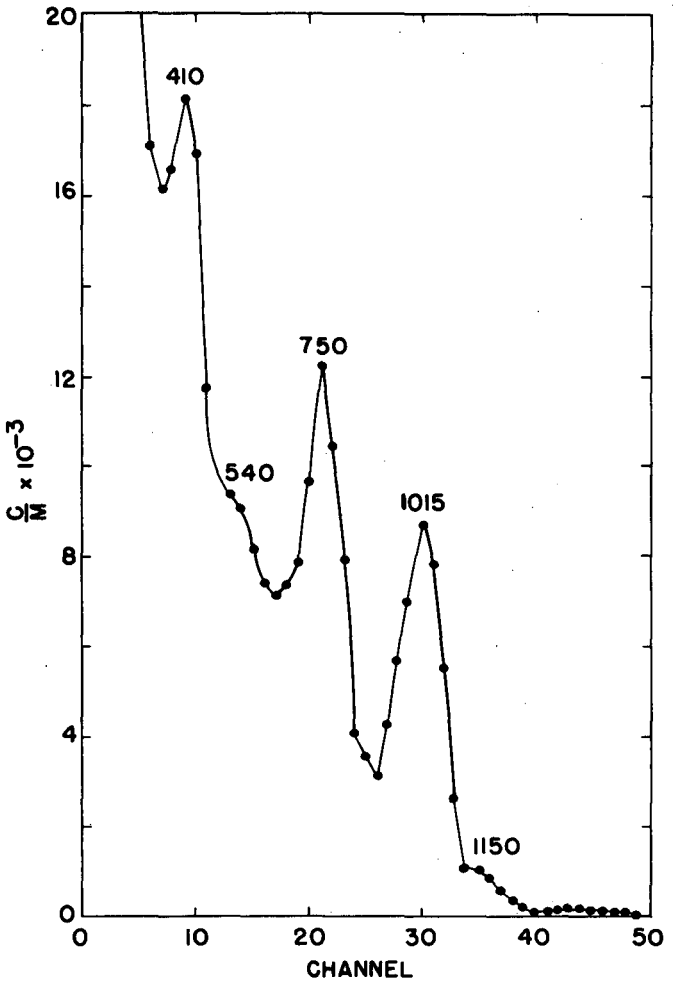


Fig. 7. Gamma spectrum of Po^{207}.

Table VII

Low Energy Internal Conversion Electrons in the Decay of Po^{207}

Gamma ray energy (kev)	Conversion shell	Electron energy (kev)	Relative intensity (arbitrary units)
60.0 ± 0.1	BiL_{II}	44.22	20
	BiL_{III}	46.57	20
	BiM_{II}	56.37	7.2
	BiM_{III}	56.82	6.5
	BiN_{II}	59.11	~4
	BiO_{II}	59.83	~4
249.4	BiK	158.9	11.1
297.0	BiK	206.5	8.0

The L shell conversion electrons of the 249.4- and 297.0-kev gamma radiation were too weak to be detected.

Data on the electrons observed on the magnetic-lens spectrometer are listed in Table VIII. Since the resolution obtained with the magnetic-lens spectrometer was quite low (5 percent), the L shell conversion electrons of the 297-, 629-, and 924-kev gamma rays (expected in very low abundance) would not be resolved from the low-energy tailing of the K conversion electrons of the 407-, 746-, and 995-kev gamma rays, respectively. The K conversion electrons of the low intensity, 500-kev gamma ray seen in the gamma spectrum would not be resolved from the L conversion electrons of the 407-kev

gamma ray. The conversion electron spectrum obtained on the magnetic-lens spectrometer corrected for decay is shown in Fig. 8a, b, and c. Because of the complexity of the conversion electron spectrum in the energy region 150 to 900 kev and the possibility of other polonium isotopes being present, the spectrum was observed at different times to detect the decay of the conversion electrons. This spectrum is shown in Figs. 9a and b.

Table VIII

High Energy Internal Conversion Electrons in the Decay of Po^{207}

Gamma Ray (kev)	Conversion shell	Electron energy (kev)	Relative intensity (arbitrary units)
249	BiK	158.9	11.1
	BiL	235	10.2
297	BiK	297	8.0
347	BiK	256	29
	BiL	331	4.5
407	BiK	316	100.0
	BiL	393	16
629	BiK	538	3.2
746	BiK	655	54
	BiL	732	9.5
924	BiK	833	2.2
995	BiK	904	41
	BiL	981	8.7
1153	BiK	1062	1.2
	BiL	1134	0.34

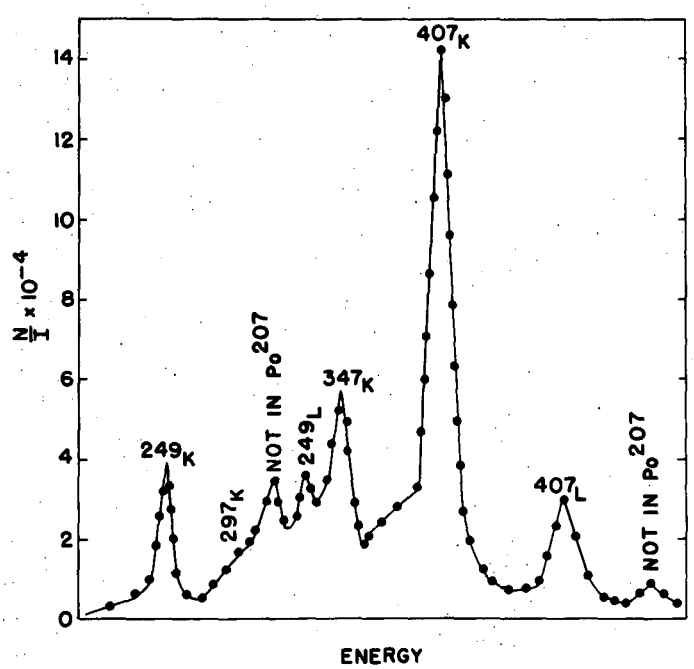


Fig. 8a. Electron spectrum of Po^{207}.

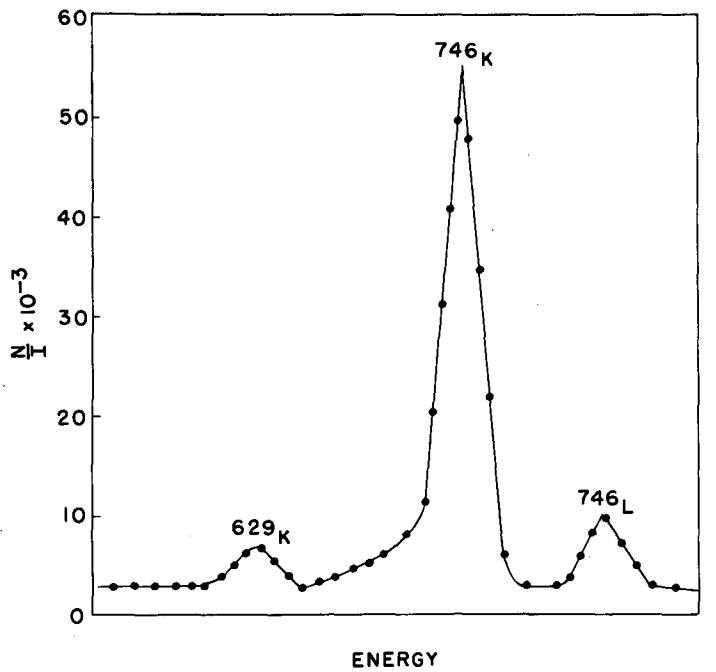


Fig. 8b. Electron spectrum of Po^{207}.

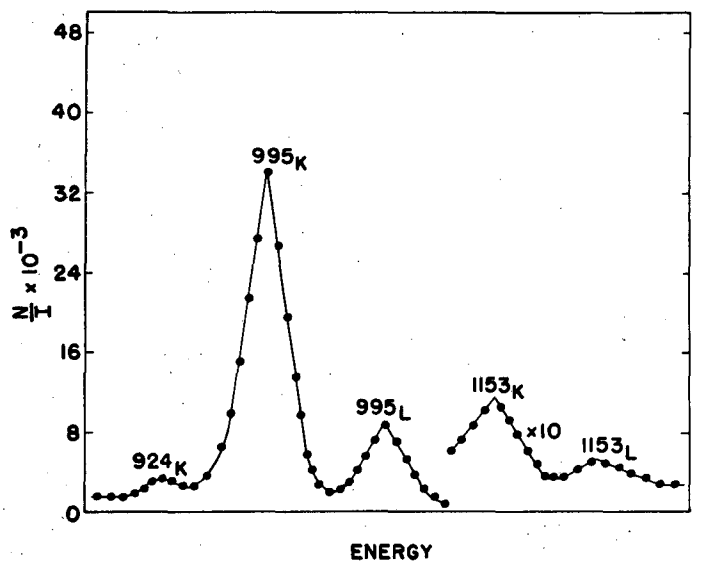


Fig. 8c. Electron spectrum of Po^{207}.

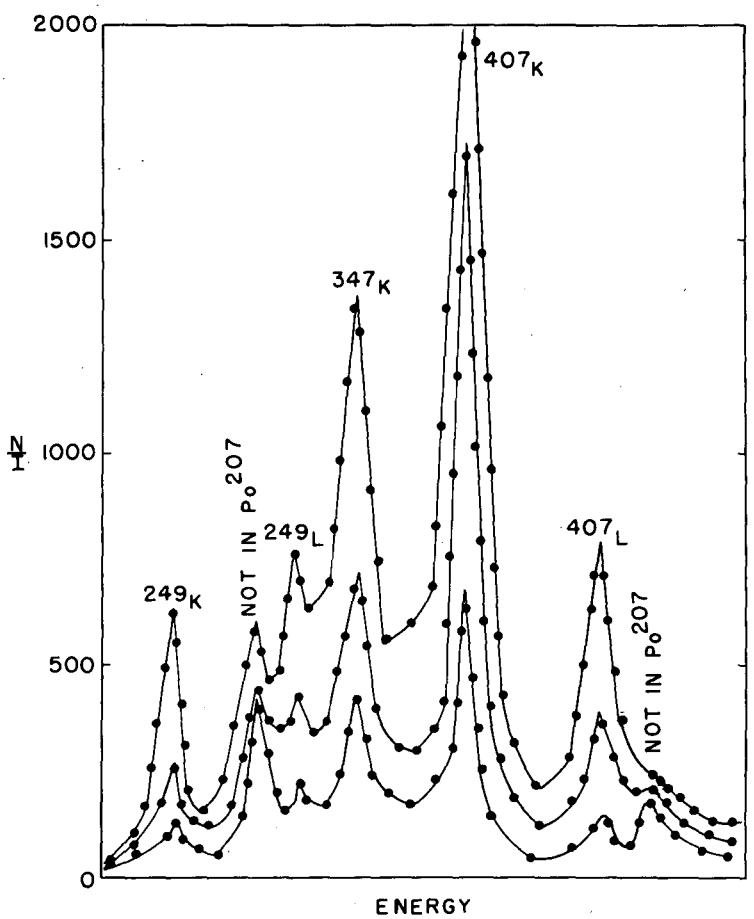


Fig. 9a. Radioactive decay of the conversion electrons of Po^{207}.

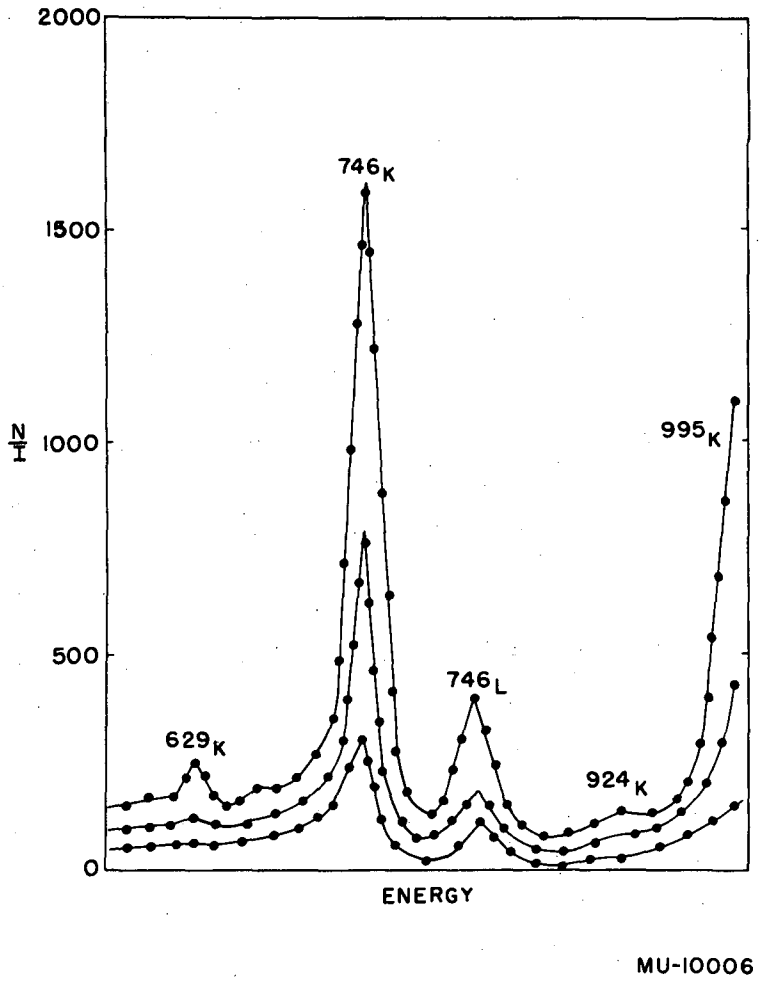


Fig. 9b. Radioactive decay of the conversion electrons of Po^{207}.

Since the K shell conversion electrons of the 249- and 297-kev gamma rays were observed on the permanent-magnet spectrograph and also on the magnetic-lens spectrometer, the relative intensities of the electrons on both spectrometers may be related to each other. The intensity of conversion electrons are listed relative to the K shell conversion electrons of the 407-kev gamma ray (100) in Tables VII and VIII.

The K/L conversion electron ratios as obtained experimentally on the magnetic-lens spectrometer are listed in Table IX together with the theoretical K/L ratios of various multipole order transitions calculated using the tables of Rose, et al.[57] The multipole order assignment favored by the experimental results of Alburger and Pryce[58] on Pb^{206} is also indicated.

On the basis of these K/L ratios it would appear that the 250- and 995-kev gamma rays are E2 transitions. The 347-, 407-, and 746-kev gamma rays cannot be assigned unambiguously from these data, but they may possibly be E1, M1, or M1(+ E2) admixtures.

The relative intensities of the 407-, 746-, and 995-kev gamma radiations for various multipole orders were calculated from the theoretical total internal conversion coefficients[57] and the relative intensities of the conversion electrons. These data are shown in Table X. The theoretical gamma-ray intensities can be compared with the experimental relative intensities listed in Table VI. The only consistent possible assignments are E2 transitions for the 995- and 746-kev gamma rays and an E2(+ M1) admixture for the 407-kev radiation. Moreover, the data would predict the 407-kev radiation to be 87 percent E2 and 13 percent M1.

Table IX

K/L Conversion Electron Ratios in the Decay of Po^{207}

Gamma ray energy	K/L Experimental	Theoretical K/L						Multipole order favored by Alburger and Pryce[58]
		E1	E2	E3	M1	M2	M3	
250	1.1	5.7	1.1	0.29	5.3	3.3	2.0	E2, E3, or M1(+ E2)
347	6.4	5.8	1.8	0.52	5.7	5.0	2.4	M1 or M1(+ E2)
407	6.2	6.2	2.3	0.80	5.7	3.9	2.9	M1 or M1(+ E2)
746	5.7	5.1	3.9	2.5	5.4	4.4	3.4	M1 or M1(+ E2)
995	4.7	5.5	4.7	3.2	5.9	4.8	4.4	E2

Table X

Theoretical Intensities of Gamma Rays in the Decay of Po^{207}

Gamma ray energy (kev)	Theoretical intensity of gamma ray (arbitrary units) (Based on relative intensity of conversion electrons) E1	E2	E3	M1	M2	M3
407	77.5	23.6	5.3	3.5	1.4	0.5
746	135	45.0	16.7	9.3	4.5	2.4
995	176	61.0	27.0	14.5	7.8	4.4

The 60-kev gamma radiation is an E2 transition also since the L_{II} and L_{III} conversion electrons as observed on the permanent-magnet spectrographs are in equal intensity while the L_I electrons are very much weaker.[17, 57] A decay scheme consistent with these data is shown in Fig. 10.

Making the assumption that there is no electron capture directly to the ground state of Bi^{207}, the population of the excited states by the capture process in Po^{207} can be estimated by a knowledge of the multipole orders of the gamma radiations and the intensities of the conversion electrons. Since the intensities of the 297-, 629-, and 924-kev gamma rays and their conversion electrons are very weak, it is estimated that there is no more than 1 percent of the electron capture populating the 3072-kev level. The 60-, 347-, 249-, and 500-kev transitions are also very weak, and it is assumed the 1495- and 2088-kev levels are not directly populated. The percentage with which each level in Bi^{207} is populated by the electron capture of Po^{207} is included in Fig. 10.

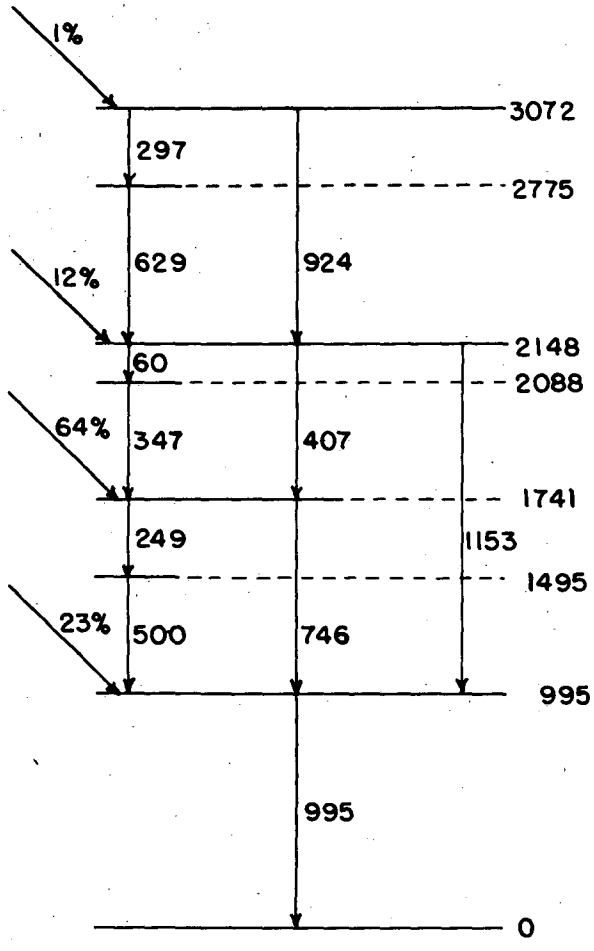


Fig. 10. Decay scheme of Po^{207}.

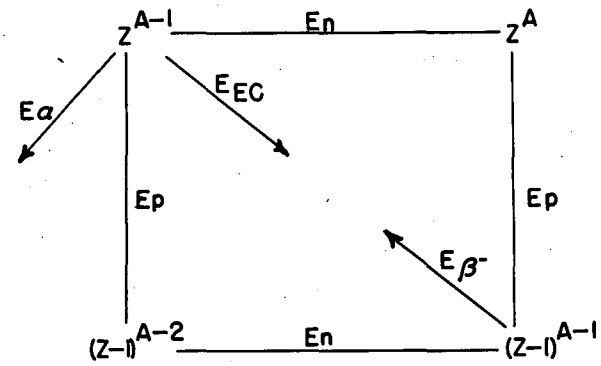
The scheme as presented requires Po^{207} to have an electron capture decay energy in excess of 3 Mev. While no closed decay energy cycles[11] are available for this region, an estimate of the decay energy can be calculated by several methods. The best estimate is probably given by the use of neutron-binding energy cycles as shown in Fig. 11a. There are two paths through which the electron capture-decay energy can be estimated using this cycle. If the neutron and proton binding energies of Z^A are known or can be estimated, the electron-capture decay energy is given by:

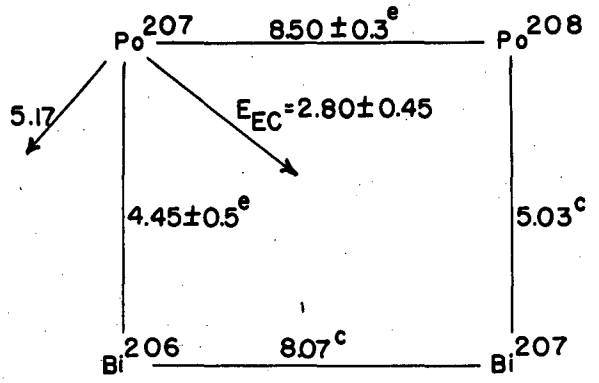
$$E_{EC} = E_{n(ZA)} - E_{p(ZA)} - (n - p) .$$

A similar path giving the same decay energy requires a knowledge of the neutron and proton binding energies of $(Z - 1)^{A-1}$ and Z^{A-1}, respectively. Again:

$$E_{EC} = E_{n[(Z-1)^{A-1}]} - E_{p(ZA-1)} - (n - p) .$$

If the neutron and proton binding energies have been calculated or estimated correctly, the electron capture-decay energy will be the same for both paths. The mass difference of the neutron and proton (n - p) is equal to 0.78 Mev. The cycles involving the electron capture of Po^{207} and Bi^{207} require a knowledge of the binding energies of the last neutron and proton in Po^{208}, the last neutron in Po^{207}, and the last proton in Bi^{207}. The neutron and proton binding energies of Po^{208} and Bi^{207}, respectively, have been calculated through their use in other cycles.[11] The neutron binding energy of Po^{208} and the proton binding energy of Po^{207} must be estimated using extrapolation of the data of Glass, et al.[11] The values used for the calculation are:





MU-10008

Fig. 11a. Neutron binding energy cycle (general).

Fig. 11b. Neutron binding energy cycle of Po^{207}.

Neutron binding energies:

$$Bi^{206-207} = 8.07 \text{ Mev (calculated)}$$

$$Po^{207-208} = 8.50 \pm 0.3 \text{ Mev (estimated)}$$

Proton binding energies:

$$Bi^{207-208} = 5.03 \text{ Mev (calculated)}$$

$$Bi^{206-207} = 4.45 \pm 0.5 \text{ Mev (estimated)}$$

The neutron binding energy cycle used for the estimation of the electron-capture decay energy of Po^{207} is shown in Fig. 11b. The value of the electron-capture decay energy is calculated to be 2.80 ± 0.45 Mev. The energy necessary for the electron-capture decay of Po^{207} (3.09 Mev) as required by the decay scheme is within the calculated limits. It would appear that the total decay energy is approximately 3.15 Mev.

Other estimates of the decay energy of Po^{207} are given by Bohr-Wheeler parabolas[11] which involve large uncertainties in this case because of the closed shell effects. Po^{207} has two protons in excess of the 82-neutron closed shell and three neutrons less than the 126-neutron closed shell. Estimates of the energy using Bohr-Wheeler parabolas give 3.5 ± 2 Mev as the decay energy. Using beta systematics[11] with constant Z, a value of 3.5 ± 0.5 is obtained for the decay energy.

4. Em^{211}

Em^{211} was first produced by Momyer[24, 25] in bombardments of thorium foils with 340-Mev protons. The mass assignment was made by observing the growth of the electron-capture daughter, At^{211}. Two

alpha group energies of 5.847 and 5.778 Mev were measured together with their abundances, 35 and 65 percent, respectively. The observed half-life of Em^{211} was 16 ± 1 hour, and the electron-capture/alpha emission branching decay ratio was 2.8 ± 0.3. Electromagnetic radiations of 65, 80, and 150 kev were observed in high abundance, and weaker 400- and 600-kev radiations were detected and assigned to Em^{211} by virtue of their 16-hour half-life.

Stoner and Asaro[61] have investigated the alpha emission branching of Em^{211} more thoroughly. Alpha particle-gamma radiation coincidence studies revealed three gamma rays, 69, 154, and 254 kev, to be in coincidence with alpha particles. Subsequently, on the alpha-particle spectrograph, a third alpha group of 5.615 Mev was detected in 1.5 percent abundance.

In the present study, Em^{211} was produced by bombarding thorium with 340-Mev protons and collecting the Em^{211} on 15-mil wires or aluminum plates by a glow-discharge technique.[24]

The electromagnetic radiations were observed on a sodium iodide (thallium-activated) crystal spectrometer. A sample spectrum is shown in Fig. 12a. Fig. 12b is a spectrum of the high-energy gamma radiations showing the very weak 1800-kev gamma ray, and Fig. 12c shows the 32- and 68-kev gamma rays observed on the sodium iodide crystal spectrometer. The 32-kev gamma ray was also seen on the methane proportional counter. The electromagnetic radiations observed are listed in Table XI. The relative intensities of the more prominent higher energy gamma rays are included. Because of their low abundance and the generally high Compton background, intensity data on the lower energy radiations are not listed. The 150-kev gamma

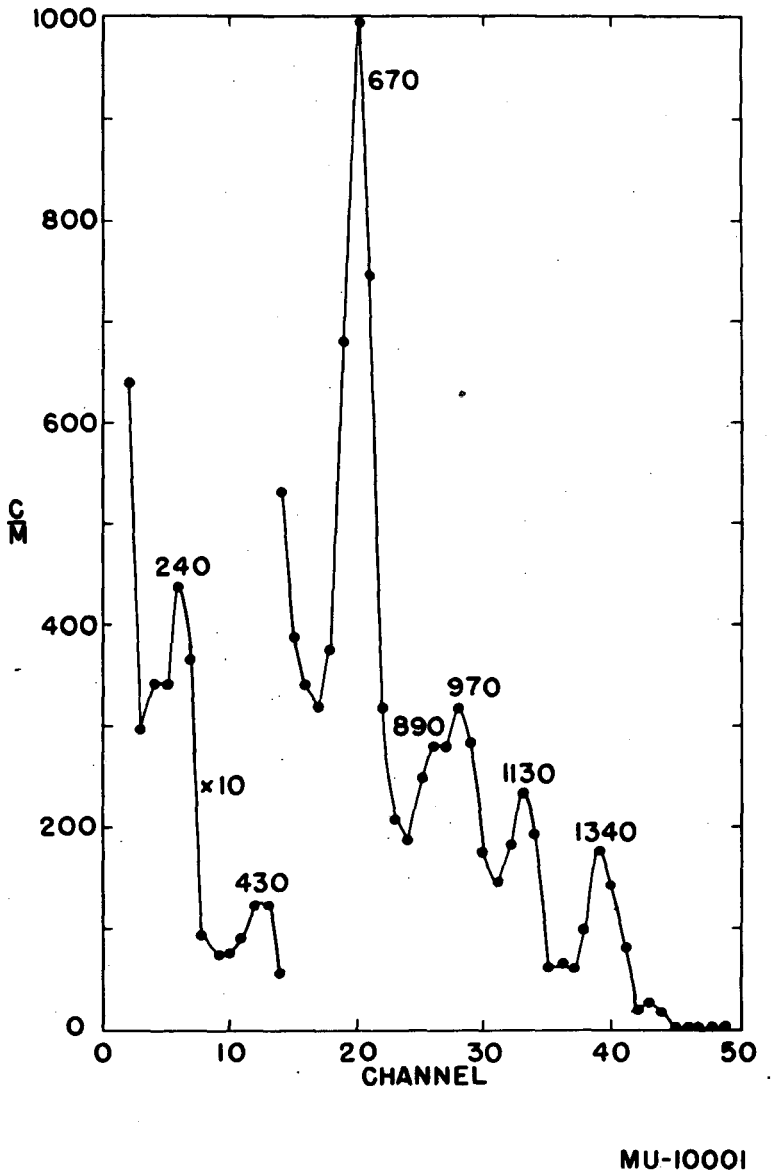


Fig. 12a. Gamma spectrum of Em^{211}.

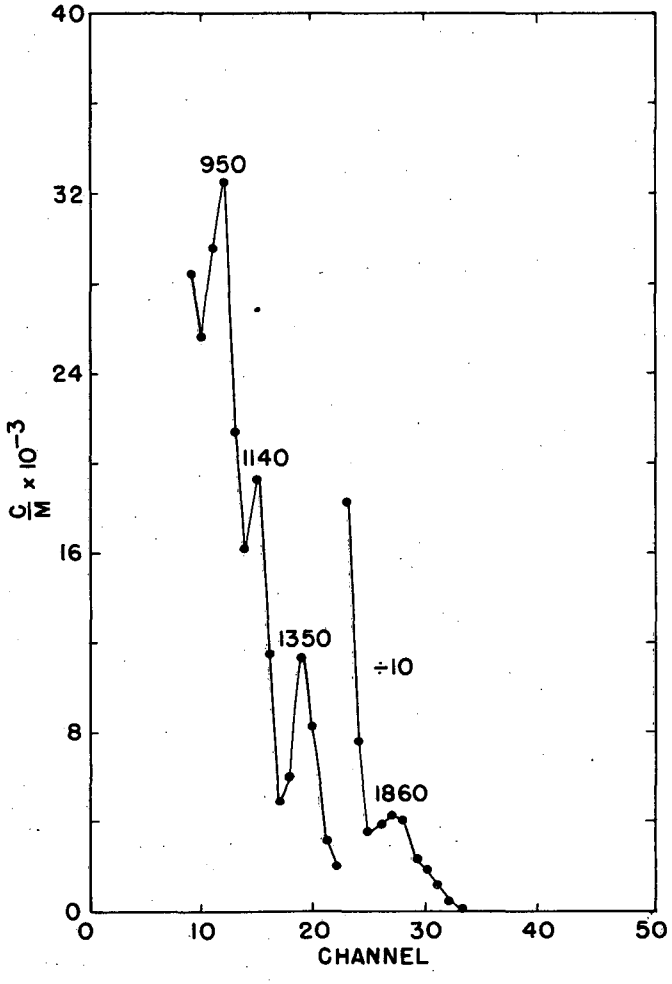


Fig. 12b. Gamma spectrum of Em^{211}.

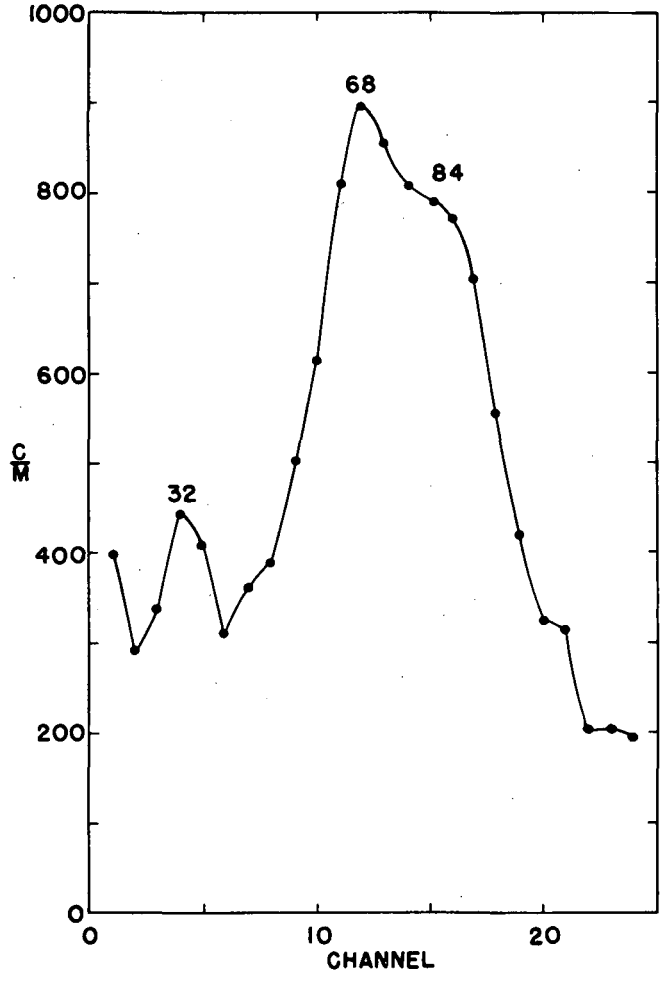


Fig. 12c. Gamma spectrum of Em^{211}.

ray reported by Momyer[24] in high abundance was not observed, although several radiations not previously reported were seen.

Table XI

Electromagnetic Radiations of Em^{211}

Gamma ray energy (kev)	Energy (arbitrary units)
32 ± 5	--
68 ± 5	--
84 ± 5 (K x-rays)	--
220 ± 20	--
320 ± 20	--
435 ± 15	39
500 ± 25	--
675 ± 15	100
870 ± 20	24
950 ± 20	29
1140 ± 20	31
1360 ± 20	52
1800 ± 50	0.8

The electromagnetic radiations in coincidence with the various gamma rays were measured. These measurements were complicated by the fact that a Compton background from the higher energy radiations is present beneath each peak and may act as the gating photon.

This makes many of the results difficult to interpret. In Table XII, the unambiguous results are listed.

Table XII

Gamma-Gamma Coincidence Studies on Em^{211}

Gating photon (kev)	Gamma rays in coincidence (kev)
435	220, 520, 670, 1140, 1360
675	430, 500, 675, 960, 1140, 1360
880-995	220, 430, 500, 670, 875
1140	220, 320, 420, 670
1360	320, 420, 520, 670

The gamma rays not listed are either not in coincidence, or the results were not readily interpretable, or the appropriate region of the spectrum was not examined. Figure 13 shows the gamma spectrum in coincidence with the 675-kev photon. Of special interest is the 675-kev gamma radiation in high abundance in coincidence with itself.

The internal conversion electrons were observed on the permanent-magnet spectrographs (20 to 250 kev) and on the magnetic-lens spectrometer (150 kev and higher). Table XIII lists the conversion electrons seen on the permanent-magnet spectrographs together with intensities. Since the L conversion electrons of the 169-kev gamma ray were seen on both instruments, all the electron intensities are listed relative to the K shell conversion electrons of the 680-kev gamma ray (100).

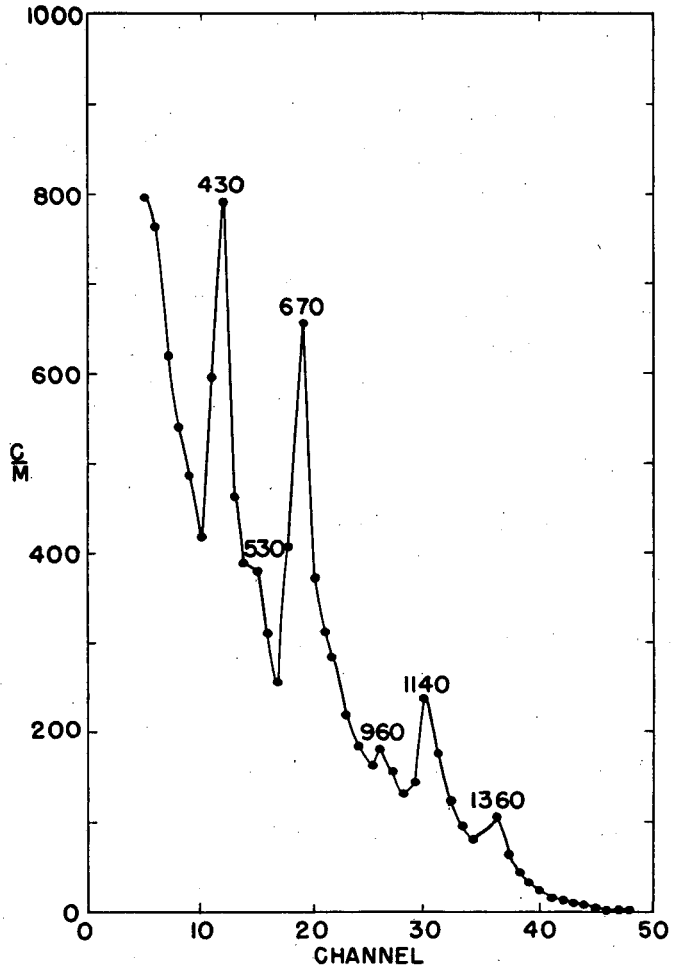


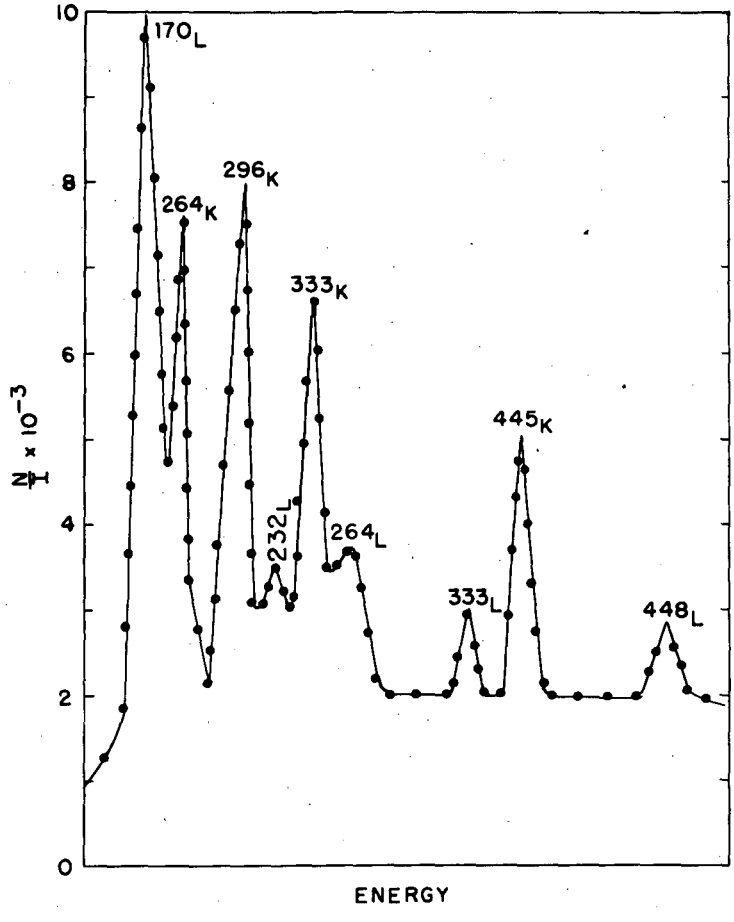
Fig. 13. Gamma rays in coincidence with 675-kev radiation.

Table XIII

Internal Conversion Electrons of Em^{211}
Observed on the Permanent Magnet Spectrographs

Electron energy (kev)	Assignment	Gamma ray energy (kev)	Relative intensity (arbitrary units)
46.39	--	--	~45
52.47	PoL_{II}	68.70	120
54.90	PoL_{III}	68.71	110
64.78	PoM_{II}	68.62	33
65.46	PoM_{III}	68.75	34
67.87	PoN_{II}	68.72	17
68.58	PoO_{II}	68.71	<10
73.18	AtK	168.91	44
151.14	AtL_{I}	168.62	<10
151.86	AtL_{II}	168.64	34
154.42	AtL_{III}	168.63	33
164.44	$AtM_{II}M_{III}$	168.5	<10
93.43	AtL_{I}	113.91	19
59-62	K-LL Auger electrons	--	<10
75-78	K-LX Auger electrons	--	<10

The conversion electron spectrum obtained on the magnetic-lens spectrometer is shown in Fig. 14a, b, and c. The electron data are given in Table XIV. The experimental K/L conversion electron ratios are listed in Table XV together with theoretical K/L ratios calculated



MU-10013

Fig. 14a. Electron spectrum of Em^{211}.

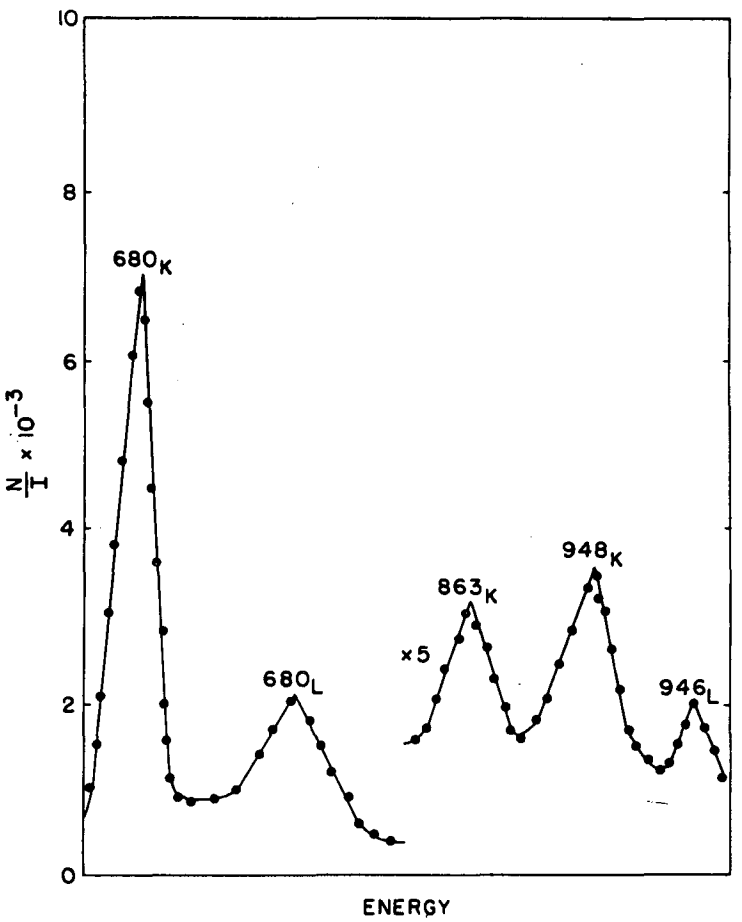


Fig. 14b. Electron spectrum of Em^{211}.

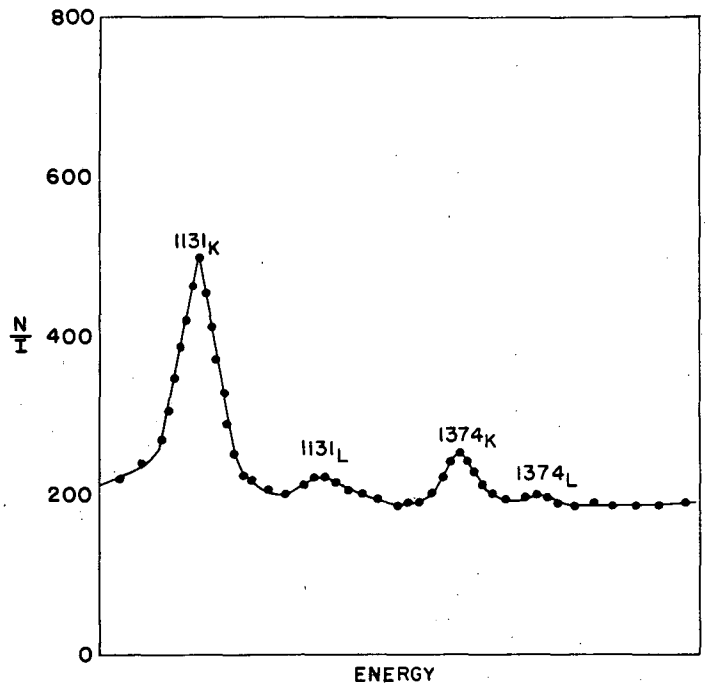


Fig. 14c. Electron spectrum of Em^{211}.

Table XIV

Internal Conversion Electrons of Em^{211}
Observed on the Magnetic-Lens Spectrometer

Electron energy (kev)	Assignment	Gamma ray energy (kev)	Relative intensity (arbitrary units)
155	AtL	170	70
200	AtK	296	48
217	AtL	232	10
256	unassigned	--	6
168	AtK	264	33
249	AtL	264	6.6
237	AtK	333	47
318	AtL	333	7.5
349	AtK	445	31
433	AtL	448	17
584	AtK	680	100
665	AtL	680	29.5
767	AtK	863	7.1
852	AtL	867	10.2
	AtK	948	
931	AtL	946	1.7
1035	AtK	1131	4.2
1118	AtL	1131	1.2
1278	AtK	1374	1.0
1359	AtL	1374	0.14

Table XV

K/L Conversion Electron Ratios in the Decay of Em^{211}

Gamma ray energy (kev)	K/L ratio experimental	Theoretical K/L ratio						Multipole order favored by Pryce and Alburger[58]
		E1	E2	E3	M1	M2	M3	
169	0.6	5.2	0.44	0.08	5.7	2.4	--	--
264	5.0	5.9	1.1	0.29	5.6	3.5	1.9	M1 or M1(+ E2)
333	6.3	5.9	1.65	0.52	5.7	3.8	2.4	M1 or M1(+ E2)
445	1.9	5.4	2.24	0.96	5.4	3.9	2.7	E2 or E3
680	3.5	5.6	3.5	2.1	4.9	4.2	3.4	E2
863	~5	5.3	4.4	2.9	5.8	4.6	3.9	E2
946	~5	5.2	4.6	3.0	5.8	4.6	4.3	E2
1131	3.6	6.5	4.6	3.5	5.8	5.2	4.6	E2
1374	≈7	--	--	--	--	--	--	E2

for various multipole orders using the theoretical conversion coefficients of Rose, et al.[57] The multipole order assignment favored by the experimental results of Alburger and Pryce[58] are included for comparative purposes.

The 68- and 169-kev gamma rays are undoubtedly E2 transitions by virtue of the relative L shell conversion electron data observed on the permanent-magnet spectrographs. The L_{II} and L_{III} shell conversion electrons are in equal abundance, while the L_I shell conversion electrons are in much lower abundance.[17, 57] Assignment of the other gamma radiations cannot be made unambiguously. The K/L ratios suggest that the 445- and 680-kev radiations are also E2 transitions, and the other gamma rays are M1(+ E2) admixtures. From the relative intensities of the conversion electrons and the total conversion coefficients for various multipole order transitions the theoretical intensities of the gamma rays can be calculated and compared with the experimental values. Since intensity ratios must be used, as only relative intensities are known, only those gamma rays whose intensities are listed in Table XI can be compared. The only seemingly consistent results obtainable by this method are made if it is assumed that the 445-kev gamma ray is an E2 transition (a probable assignment on the basis of the K/L ratio). If the 445-kev radiation is E2, then the 865- and 1131-kev gamma rays are E2 also, and the 946-kev radiation is an M1(+ E2) admixture. The 680-kev gamma ray would be an M2 transition if only one gamma ray of that energy were present. However, since 680-kev radiation in high abundance is found in coincidence with itself, it appears that two gamma rays of very nearly identical energies are present, and hence the multipole order assignment above is not meaningful.

Before attempting to present an electron-capture decay scheme for Em^{211}, it would be well to point out the following sums, which should be useful in the construction of a decay scheme.

$$1820 + 0 = 1820 \qquad 1131 + 680 = 1811$$

$$1374 + 445 = 1819 \qquad 865 + 946 = 1811$$

The six gamma rays, with the exception of the very weak 1800-kev radiation, are the most abundant radiations observed, and although an unambiguous decay scheme probably cannot be presented, it is believed that these seven gamma rays in the sums above constitute the correct skeleton. The 68.70-kev gamma ray occurs in the alpha-particle emission branching of Em^{211} to Po^{207} as evidenced by the addition of polonium electron binding energies to the conversion electron energies. The two main alpha groups of 5.847 and 5.778 Mev are separated by 69 kev. While the third alpha group decays to a state 232 kev above the ground state of Po^{207}, it would appear that most of the 232-kev radiation observed belongs in the electron-capture branching because of intensity considerations. The third alpha group is present in only 1.5 percent abundance, and the intensity of the 232-kev radiation observed is very much higher. Since there apparently are two 680-kev transitions with very nearly identical energies and the gamma-gamma coincidence studies indicate that all the more abundant radiations are in coincidence with a 680-kev photon, it is suggested that one of the 680-kev gamma rays is a ground state transition while the major skeleton mentioned above lies above it. A decay scheme consistent with these data is shown in Fig. 15. The major skeleton of the decay scheme, containing most of the more abundant radiations, is shown in solid lines. The radiations which are quite ambiguous

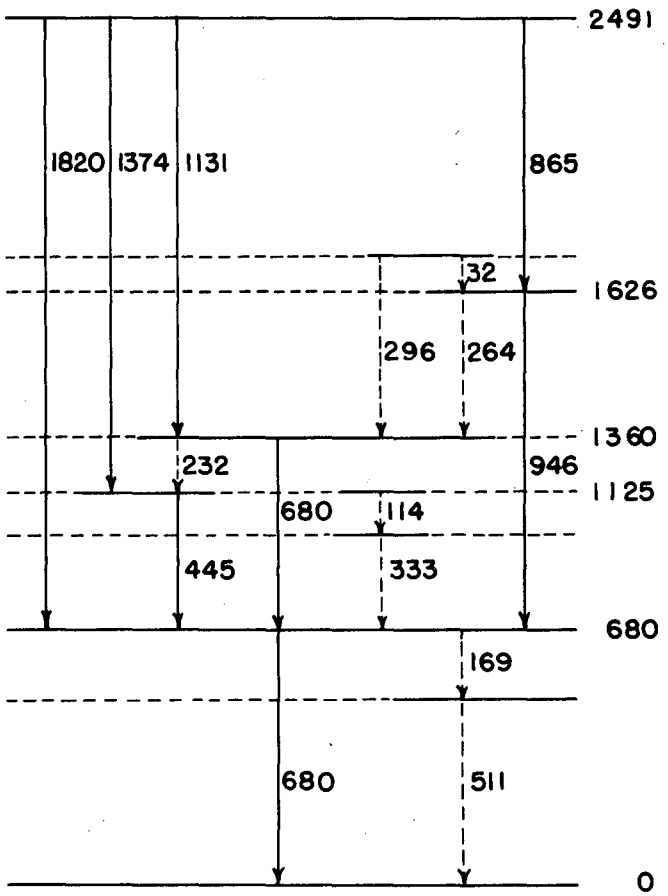


Fig. 15. Energy levels of At^{211}.

are shown with dotted lines. These dotted transitions indicate only a possible scheme, many others being conceivable.

From the data available, estimates of the relative population of the levels of At^{211} by the electron capture of Em^{211} are not possible. However, since the 1374-, 1131-, and 865-kev transitions are in high abundance, the relative population of the 2491-kev level must be high, possibly 75 percent.

Again, the total electron-capture decay energy of Em^{211} can only be estimated by the use of neutron-binding energy cycles.[11] The cycle which includes the electron capture of Em^{211} is shown in Fig. 16. The proton and neutron binding energies of Em^{212} and At^{211}, respectively, have been calculated through their use in other cycles. However, either the neutron binding energy of Em^{212} or the proton binding energy of Em^{211} must be estimated before the electron-capture decay energy of Em^{211} can be evaluated. Using the data compiled by Glass, et al.,[11] the values used in the calculation are:

Neutron binding energies

$At^{210-211}$ = 7.72 Mev (calculated)

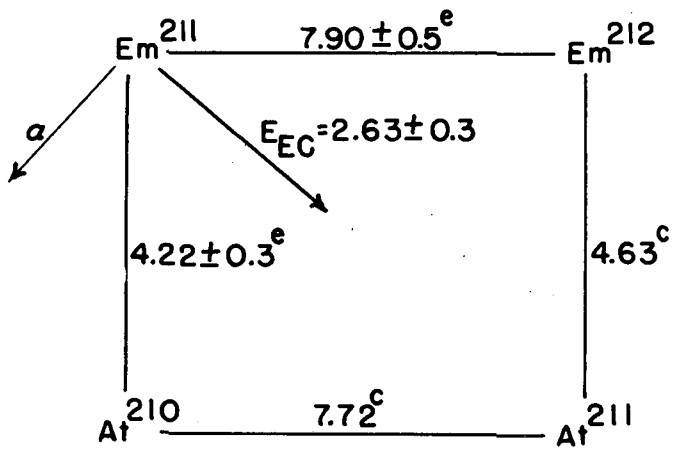
$Em^{212-213}$ = 7.9 ± 0.5 Mev (estimated)

Proton binding energies

$At^{211} - Em^{212}$ = 4.63 Mev (calculated)

$At^{210} - Em^{211}$ = 4.22 ± 0.3 Mev (estimated).

The estimated electron-capture decay energy of Em^{211} using these neutron binding energy cycles is 2.63 ± 0.3 Mev. The decay scheme as presented in Fig. 15 requires a decay energy of at least 2.51 Mev, within the limits of the estimated decay energy.



MU-10017

Fig. 16. Neutron binding energy cycle of Em^{211}.

A general decay scheme showing the genetic relationships of Em^{211} which lead finally to stable Pb^{207} and Tl^{203} is shown in Fig. 17.

5. At^{209}

An activity characterized by a 5.5-hour half-life and an alpha particle of 5.65 Mev was assigned to At^{209} by Barton, et al.[21,62] The alpha particle emission/electron capture branching ratio was estimated as 0.05. Mihelich, et al.[27] observed conversion electrons from gamma rays of 83.8, 91.1, 195, 548, and 784 kev, which were assigned to At^{209} by virtue of their 5.5-hour half-life.

In the present study a source of At^{209}, prepared by the bombardment of bismuth with 46-Mev helium ions, was examined on the alpha-particle spectrograph. Hoff, et al.[63] had previously studied At^{209} on this instrument, but because of insufficient activity (50 alpha tracks (5.642 Mev) attributable to At^{209} were observed) nothing was determined of the alpha fine structure. In order to establish whether the gamma radiation should be assigned to the electron-capture branching decay of At^{209}, the presence or absence of complex structure in the alpha-particle emission must be ascertained.

Two exposures were made of the At^{209} alpha spectrum on the alpha-particle spectrograph. The first exposure contained 5600 tracks due to a 5.642-Mev alpha group, and the second exposure of the same sample taken approximately 12 hours later contained 2000 tracks due to an alpha group of 5.642 Mev. Since At^{210} was produced in the bombardment also, the energies of the At^{210} (5.519, 5.437, and 5.355 Mev) and Po^{210} (5.298 Mev) alpha tracks were used as internal standards of the energy. The alpha spectrum obtained in the second

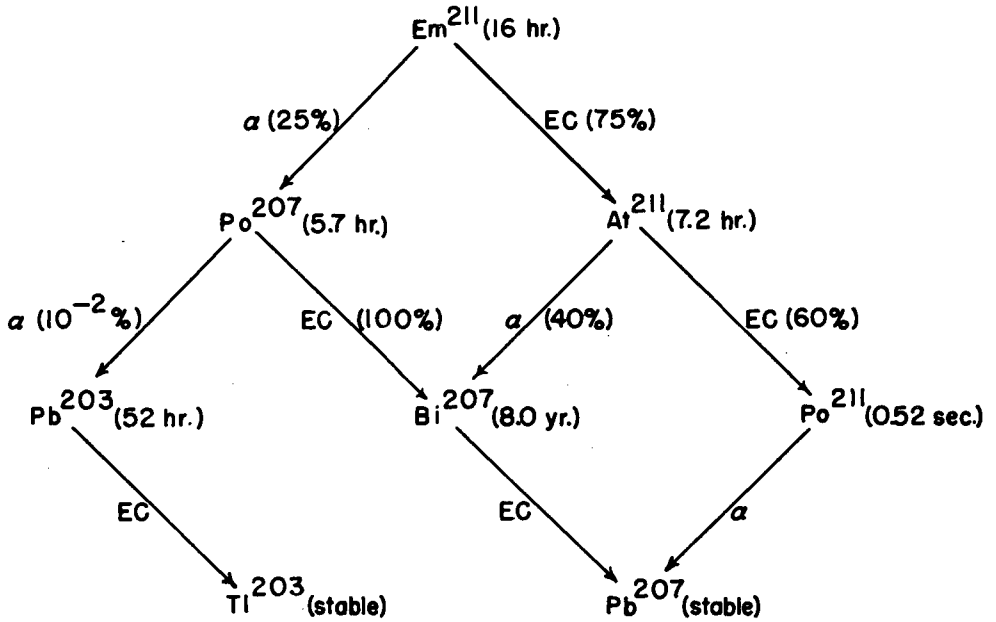


Fig. 17. General decay scheme of Em^{211}.

exposure is shown in Fig. 18. A limit of 2 1/2 percent of the total alpha disintegrations can be set for the presence of other alpha groups in the alpha branching decay of At^{209} unless their energies correspond to the same energies of the alpha groups of At^{210} and Po^{210}. Therefore, all the gamma radiations observed in the decay of At^{209} seem to occur in the electron-capture branching decay to Po^{209}.

IV. DISCUSSIONS

A. The Auger Effect

The first attempt to outline a theory of the Auger effect was by Wentzel[65] in 1927. Using a two-electron atom of high nuclear charge, Wentzel was able to show that the reciprocal of the lifetime of a K shell vacancy with respect to an Auger transition in which an L electron is emitted should be independent of Z. Since the reciprocal of the effective life of an excited K state with respect to radiation of x-rays is approximately proportional[1] to Z^4, W_K, the K fluorescence yield may be expressed as:

$$W_K = Z^4/k + Z^4 .$$

Such an expression, however, can only be qualitatively correct because any complete and accurate theory of the Auger effect would be based on a proper theory of quantum electrodynamics since the effect involves the interaction of several electrons[66] rather than only two. Such a theory in a satisfactory state does not exist at present.

Using the expressions derived by Wentzel,[65] calculations of the fluorescence yield have been made by Burhop[67] and Pincherle[68] using a nonrelativistic theory and by Massey and Burhop[69] using a relativistic theory. In these calculations, hydrogen-like, single-

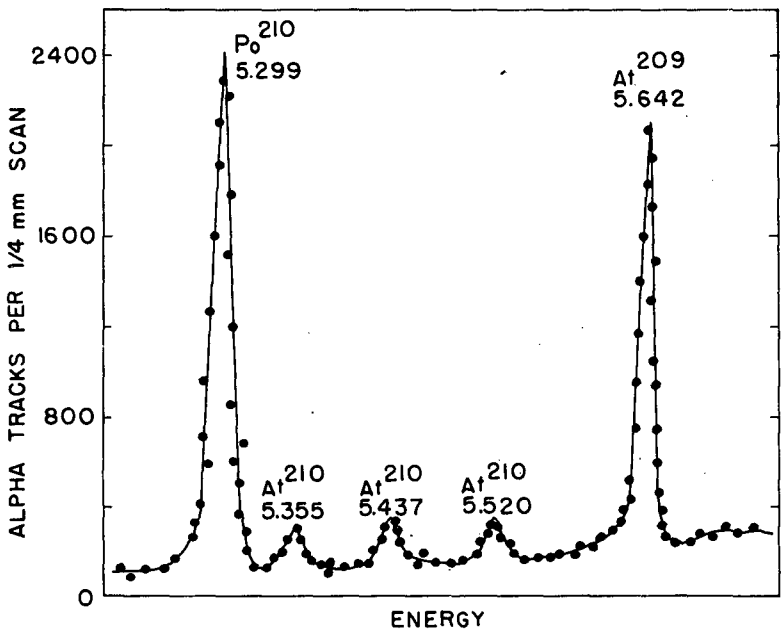


Fig. 18. Alpha spectrum of At^{209}.

electron wave functions were used, the effective nuclear charge being determined by the application of Slater's rules.[70] The use of screened, hydrogen-like wave functions in the relativistic calculations increases the calculated Auger probability for elements of high atomic number. The calculations involved are very laborious and have only been carried out for a few cases. The relativistic value of the K Auger yield for mercury for example, is 0.06 while the nonrelativistic value is only one-half as great, or 0.03. Relativistic effects are of some importance for elements of atomic number as low as 47 where the relativistic value of the Auger yield is still approximately 20 percent larger than the nonrelativistic value.

Table XVI compares the experimental values of the Auger yield of ytterbium, polonium, and uranium with the calculated theoretical values of Massey and Burhop.[69] The experimental results are only in qualitative agreement with the theoretical values as was expected. Until a more accurate theory of the Auger effect becomes available, quantitative agreement will probably not be possible.

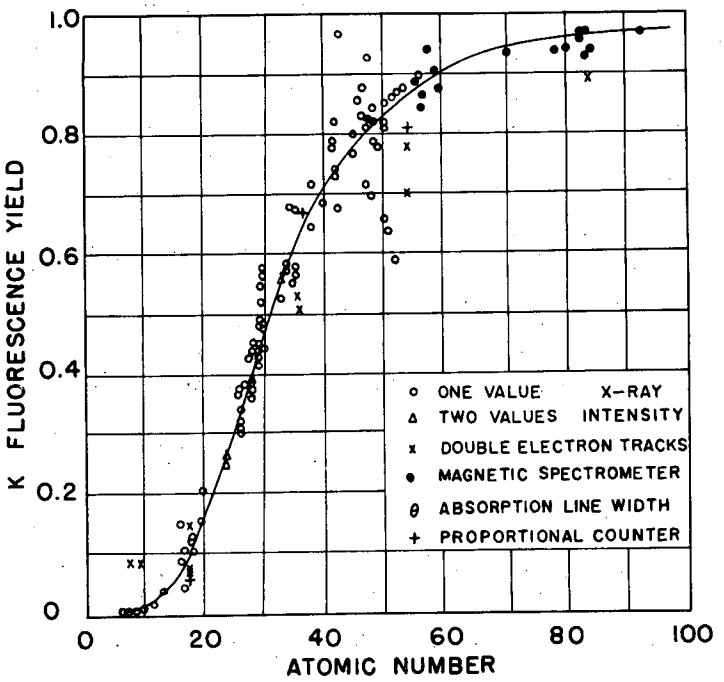
Table XVI

Comparison of the Experimental and Theoretical Values of the Auger Yield of Ytterbium, Polonium, and Uranium

Element	Atomic number	Auger yield experimental	Auger yield theoretical[69]
ytterbium	70	0.06	0.08
polonium	84	0.06 (upper limit)	0.045
uranium	92	0.03	0.04

Several summaries of the magnitude of the Auger effect have been published. The summaries of Arends[71] in 1935 and Backhurst[72] in 1936, for example, cover the contemporary data on fluorescence yields very well but do not include any measurements on the heavier elements. Not until the complete summaries of Burhop[73] (data though 1950) and Broyles, et al.[2] became available did the first collected data on elements of atomic number greater than 56 appear. A new, and it is hoped, complete summary of the data through June 1955 is given in Fig. 19. Since the only new data are for elements with atomic numbers 56 and larger, a complete reference list is not included as Broyles, et al.[2] have covered the reference material of their available data very thoroughly. The new values of the fluorescence yields for elements heavier than cesium (Z = 55) are listed in Table XVII. The value is followed by a lower-case letter referring to a list of workers who obtained these values and an indication of how the measurements were made.

A least-squares fit to all these data would require a study of all the methods used so that proper weights could be assigned to the different values. This has not been attempted here, but an estimated curve has been drawn through the points taking into consideration the estimated reliability of the various values. Below Z = 50 the curve is essentially the same as that presented by Broyles, et al.,[2] and their analyses of the reliability of the values will suffice here also. Above Z = 50 the curve varies slightly from Broyles, et al. because of the additional data on this heavy element region which has become available.



MU-10020

Fig. 19. Graphical summary of fluorescence yields.

Table XVII

Recent Data on Fluorescence Yield Values

Element	Atomic number	K fluorescence yield	Reference
barium	56	0.85	a
lanthanum	57	0.94	b
cerium-praseodymium	58-59	0.90	c
ytterbium	70	0.94	d
lead	82	0.96	e
bismuth	83	0.96	f
polonium	84	0.94	g
uranium	92	0.97	g

a. T. Azuma, J. Phys. Soc. Japan 9, 443 (1954), conversion electrons; magnetic spectrometer.

b. C.H. Pruett and R.G. Wilkinson, Phys. Rev. 96, 1340 (1954); conversion electrons, electron capture isotope, magnetic spectrometer.

c. C.I. Browne, J.O. Rasmussen, J.P. Surls, and D.F. Martin, Phys. Rev. 85, 146 (1952); electron capture isotope, magnetic spectrometer.

d. This work, conversion electrons, magnetic spectrometer.

e. A.H. Wapstra, Ph.D. Thesis, University of Amsterdam (published by G. van Soest, Amsterdam, 1953); electron capture isotope, conversion electrons, magnetic spectrometer.

f. M. Mladjenovic and H. Slätis, Arkiv för Fysik 9, 41 (1955); conversion electrons, magnetic spectrometer.

g. This work, electron capture isotope, magnetic spectrometer.

The experimental values support in a qualitative way the theoretical variation of the fluorescence yield with atomic number, but none of the curves yet suggested, theoretical or semiempirical, is in satisfactory agreement with all the data. The relation

$$W_K = 0.957Z^4(0.984 \times 10^6 + Z^4)^{-1}$$

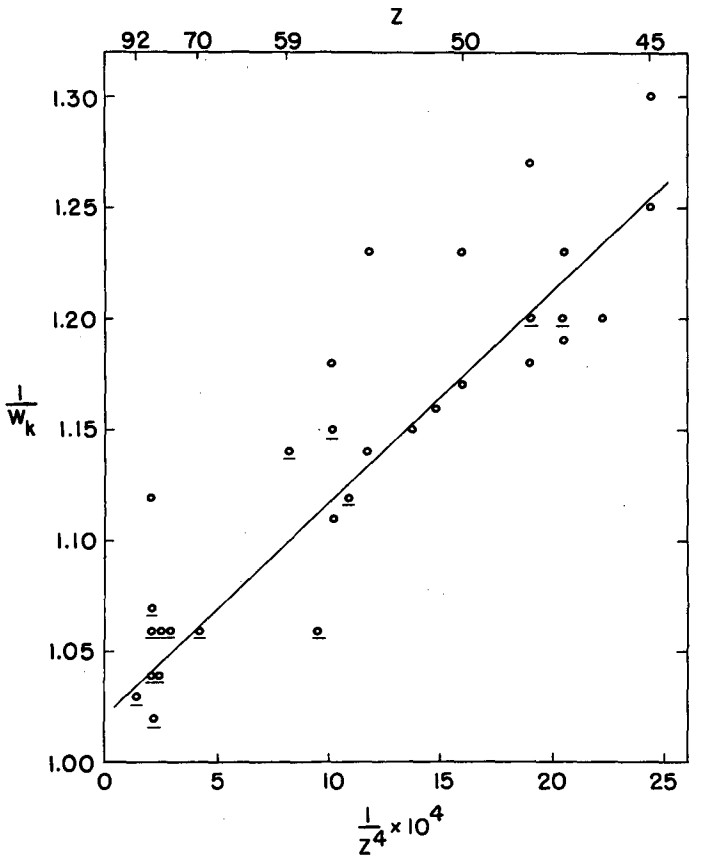
given by Arends[71] and recommended by Tellez-Plascencia[74] gives the best fit of those that have been proposed. If an expression of the form

$$W_K = AZ^4(b + Z^4)^{-1}$$

is valid, a plot of $1/W_K$ versus $1/Z^4$ should be linear with a slope of (b/a). As shown in Fig. 20 the experimental results are well represented by a straight line drawn through the most reliable of the experimental values. The values of a and b which best represent the experimental points are 0.98 and 0.98×10^6, respectively. The expression of the K fluorescence yield then becomes:

$$W_K = 0.98Z^4(0.98 \times 10^6 + Z^4)^{-1}.$$

Since the available theory and experimental results on K fluoresence and K Auger yields agree that for elements of low atomic number $W_K << 1$ and $a_K \approx 1$ and for elements of high atomic number $W_K \approx 1$ and $a_K << 1$, it would appear that the direct measurement of the K Auger yield would be more accurate than a direct determination of the fluorescence yield for elements of atomic number greater than 30 since $a_K > 0.5$ for these elements. In general, this has been done experimentally and exclusively for elements of atomic number greater than 56. It is believed that the magnetic spectrometer measurements are the most accurate for the region in which they have been made.



MU-10021

Fig. 20. Variation of $1/W_K$ with $1/Z^4$ in the heavier elements.

These data are indicated by underlining the experimental points in Fig. 20.

In addition to the values of the K fluorescence yields there are sufficient experimental measurements of the K-LX to K-LL Auger electron intensity ratios available to indicate approximately the variation of this ratio with atomic number. The available data on the Auger electron intensity ratios are listed in Table XVIII and shown graphically in Fig. 21. It is interesting to compare these experimental ratios of the intensities of the groups of Auger electrons to those obtained from the calculated probabilities of Pincherle[68] using the expressions derived by Wentzel.[65] This calculated intensity ratio is K-LL:K-LX = 1.00:0.716 and should be independent of atomic number. As seen from Fig. 21, the experimental ratios are not constant, but appear to increase with increasing atomic number. For the heavier elements, the ratios approach the value obtained by Pincherle when transition probabilities are used.

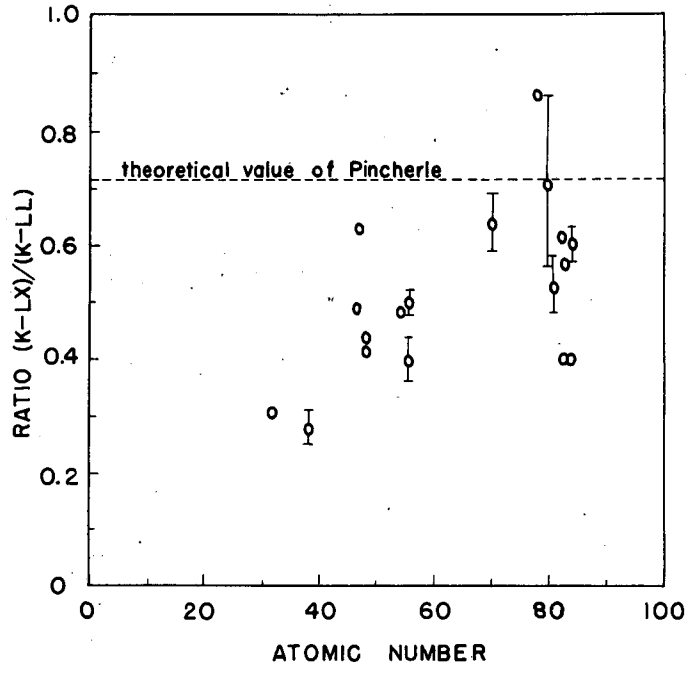
It may be of interest also to compare the values of the relative intensities of the individual K-LL Auger electrons of polonium with the other available data as well as with the theoretical relativistic intensities of Massey and Burhop[69] and the nonrelativistic calculations of Burhop.[67] This comparison is given in Table XIX.

The experimentally determined relative intensities of polonium are not in agreement with the theoretical predictions but agree fairly well with the other heavy element values. The values calculated by Burhop[67] are for Z = 47 but should be almost independent of Z in the nonrelativistic theory. It is apparent, however, that the experimental results of Johnson and Foster[78] for Z = 47 are in somewhat better agreement with

Table XVIII

Experimental Ratios of K-LX to K-LL Transitions as Measured by Various Observers

Element	Atomic number	K-LX/K-LL	Reference
germanium	32	0.31	75
strontium	38	0.28	76
silver	47	0.49	77
silver	47	0.63	78
cadmium	48	0.44	77
indium	49	0.42	2
cesium	55	0.48	79
barium	56	0.4	2
barium	56	0.5	80
ytterbium	70	0.64	81
platinum	78	0.56	82
mercury	80	0.71	2
mercury-thallium	80-81	0.53	17
bismuth	83	>0.4	83
bismuth	83	>0.57	84
bismuth	83	0.64	44
polonium	84	0.4	26
polonium	84	0.55	81
theoretical value for all atomic numbers:		0.716	68



MU-10022

Fig. 21. Graphical summary of the ratio of K-LX to K-LL Auger transitions.

Table XIX

Experimental and Theoretical Relative Intensities of K Auger Lines

Element	Z	K Auger Lines						Reference
		$K\text{-}L_IL_I$	$K\text{-}L_IL_{II}$	$K\text{-}L_IL_{III}$	$K\text{-}L_{II}L_{III}$	$K\text{-}L_{III}L_{III}$	$K\text{-}L_{II}L_{II}$	
silver	47	1.0	1.3	1.3	3.2	1.8	0.5	78
xenon	54	weak	moderate	moderate	strong	moderate	--	19
gold	79	1.0	1.7	1.2	1.4	0.8	0.3	85
mercury	80	1.0	1.2	0.7	1.4	0.6	0.2	38
bismuth	83	1.0	1.8	1.1	1.6	0.8	<0.2	44
bismuth	83	1.0	1.8	1.3	2.3	1.3	<0.2	86
polonium	84	1.0	1.4	0.6	1.3	0.7	<0.1	81
theoretical nonrelativistic		1.0	1.13	2.26	4.03	2.30	0.38	73
theoretical relativistic	79	1.0	5.5	5.3	--	--	--	69

these nonrelativistic intensities than are the values of the heavier elements.

B. Electron Capture

Before a correlation of the experimental results with the theoretical aspects of electron capture can be made, Fermi's theory of beta decay[87] must be introduced. The lifetimes of nuclei which are unstable towards beta decay are governed by selection rules which depend upon the spin and parity of the initial and final nucleus. Since the half-lives of beta-decaying isotopes depend sensitively on the energy available in the process, the half-lives alone do not reflect these selection rules. Fermi, however, introduced a function $f(Z, E_\beta)$, dependent on the charge Z and the maximum kinetic energy of the electron or the neutrino energy in the electron-capture process, such that the product ft of this function with the half-life, t, is a measure of the matrix element and the strength of the interaction. The theoretical approach involved a point interaction between the neutrons and protons and the electron and neutrino fields in the form of products of the nucleon, electron, and neutrino wave functions, and an interaction constant, G. Such products of the four compoent relativistic wave functions, using the four-dimensional Dirac matrices, α and β, can be formed in several ways. However, according to the Dirac theory only five different expressions are relativistically invariant.[88] These are usually called the scalar, polar vector, tensor, axial vector, and pseudoscalar interactions. These interactions give rise to different selection rules. The selection rules following from scalar interaction, where the nucleon does not change its spin in a beta

transformation, were considered by Fermi. However, there is good evidence that these selection rules are not always followed. Gamow and Teller[89] were the first to consider the tensor interaction in a modification of Fermi's theory in which a spin change of the nucleon can occur in an "allowed" transition.

Briefly, for allowed transitions, the probability P(W) of emission of an electron with energy W must have the form:

$$P(W)dW = g^2 |M|^2 F(Z, W) W(W^2 - 1)^{1/2}(W - W_\beta)^2 \, dW \, .$$

Here, g should be constant, the same for all transitions. It depends on various fundamental constants and is a measure of the strength G of the interaction. M is the nuclear matrix element and F(Z, W) is the square of the value of the relativistic eigenfunction of the electron in the Coulomb field of the nucleus at the origin. F(Z, W) depends on the energy W and the charge Z. The total transition probability, and thereby the lifetime, is obtained by integrating the above equation over all possible energies from 1 to W_β, the energy of the most emergetic electron. This integral is denoted by $f(Z, W_\beta)$ and:

$$f(Z, W_\beta) = \int_1^{W_\beta} F(Z, W)(W^2 - 1)^{1/2}(W_\beta - W)^2 W dW \, .$$

The function f increases rapidly with increasing endpoint energy, W_β. It can be evaluated numerically for all values of Z, and it depends on Z and the maximum kinetic energy E_β only. The half-life, t, is then obtained by:

$$\ln 2/t = |M|^2 g^2 f(Z, E_\beta) \, .$$

The product ft is generally used in the discussion of experimental data:

$$ft = \ln 2/|M|^2 g^2 \, .$$

The ft product is then a measure of the inverse square of the matrix element and of the interaction constant. Large values of ft correspond to small matrix elements and forbidden transitions.

K electron capture is governed by the same matrix elements as beta decay. The transition probability for K electron capture depends on the energy in a different manner since the phase volume and the electron eigenfunctions are different. However, it is possible to construct analogously to the method used for beta decay a function $f_K(E, Z)$ such that $f_K t$ has the same meaning as the ft above for beta decay.[90]

It is obvious that the ft product is independent of the energy release and nuclear charge for allowed transitions. Because M has been assumed independent of the energy, the expression for ft above strictly applies only to allowed spectra. For such nuclides the product ft should be a constant. An ft value can be computed, however, for any transition of known energy and half-life. This is a useful procedure because it provides an immediate orientation as to whether the transition is allowed or forbidden. Presumably the ft values of forbidden transitions are considerably larger than those of allowed transitions. Therefore, a comparison of the "degree of forbiddenness" of different transitions can be made on this basis. Although the ft values should be a constant for a definite degree of forbiddenness, a considerable variation in the matrix elements is to be expected as a consequence of variations in nuclear structure. Nevertheless, the experimental ft values do divide into fairly distinct groups, and it is usually possible to account for the separation by assigning to each group a definite order of forbiddenness. A correction to the ft values sometimes becomes necessary if the spin of the initial nucleus is less than the spin of the level to which the

decay occurs. The ft value must then be multiplied by a statistical factor, $(2I_f + 1)/(2I_i + 1)$. In general, this will not result in an appreciable increase of the ft value.

The selection rules of Fermi and Gamow and Teller, together with the approximate ft-value groupings for the beta transitions are given in Table XX.

Calculations of ft values for electron-capture isotopes of the heavy elements have been made where the decay scheme, the electron-capture partial half-life, and the decay energy were available.

At^{211} appears to decay entirely to the ground state of Po^{211} with no transitions populating excited levels. The observed 62-kev gamma ray and 46-kev electrons are not thought to be due to At^{211} decay to an excited level in Po^{211} because of intensity considerations. The log ft value of the ground state transition was calculated to be 5.9. Although this ft value would seemingly indicate an allowed transition, it is probably first forbidden with a $\Delta I = 0, 1$ yes assignment. The ft values for transitions near closed nuclear shells (At^{211} has three protons in excess of the 82-proton closed shell and has exactly a closed shell of 126 neutrons) appear to have abnormally low ft values.

Table XX

Selection Rules for Beta Decay

Classification	Parity change	ΔI Fermi (scalar)	ΔI Gamow-Teller (tensor)	Log ft
allowed	no	0	0, 1 no $0 \rightarrow 0$	4-6
1st forbidden	yes	0, 1 no $0 \rightarrow 0$	0, 1, 2	6-8
2nd forbidden	no	1, 2	2, 3 $0 \rightarrow 0$	12 and higher

From nuclear shell model theory, decay between ground states of all nuclei heavier than mass 143 should be at least 1st forbidden since it involves a change of parity.[91] This is then consistent with our assignment of At^{211} as 1st forbidden although the ft value is slightly low. The ground state spins of At^{211} and Po^{211} have not been directly determined, but from nuclear shell model considerations, the assignment of $h_{9/2}$ and $g_{9/2}$ to At^{211} and Po^{211}, respectively, appear reasonable.

Eighty percent of the electron-capture transitions of Np^{236} decay to the ground state and 20 percent to a 44-kev level of U^{236}. The log ft value for the ground state transition is 7.0 which is consistent with a $\Delta I = 0, 1$ yes type of transition. This is in agreement with the requirement noted above that decay between ground states should be forbidden. The log ft of the transition to the excited level is 7.6, again consistent with a $\Delta I = 0, 1$ yes assignment. Since the electron-capture daughter of Np^{236}, U^{236}, has an even-even nucleus, the spins and parities of the ground state and first excited level are 0+ and 2+, respectively.[92] Therefore, a suggested assignment of the spin and parity for the ground state of Np^{236} is 1-.

Po^{207} decays to highly excited levels of Bi^{207}. The three excited levels of Bi^{207} populated to the largest extent have log ft values (beginning with the lowest-lying populated state) of 7.1, 6.3, and 6.7, respectively. These ft values are consistent with $\Delta I = 0, 1$ yes assignments. The 3.1-Mev level of Bi^{207} is only populated by approximately 1 percent of the transitions. This small population coupled with the uncertainty of the decay energy available (it is not known definitely whether enough energy is available for K electron capture as well as L electron capture since the decay energy was estimated from neutron

binding energies) makes an estimation of the log ft value for this transition meaningless.

Intensity considerations indicate that all or most of the electron-capture decay of Em^{211} proceeds to the 2.5-Mev level of At^{211}. Since there is an uncertainty in the decay energy available for the electron-capture decay of Em^{211}, the energy of the neutrino emitted is not well defined. Because of these limitations, the log ft value cannot be calculated precisely, but appears to be less than 5.5. This would indicate that the Em^{211} electron-capture decay is allowed.

Thompson[12] and Feather[13] in early studies of the electron-capture process in the heavy elements attempted to classify a number of electron-capture isotopes according to the allowed or forbidden nature of their transitions by plotting the partial half-lives as a function of energy. Their correlations, however, were very limited by a lack of experimental data. Major and Biedenharn[15] have extended these studies to the lighter nuclei whenever data were available. They conclude that the scatter of data on such a diagram does not permit the differentiation into degrees of forbiddenness. More recently, Glass, et al.[11] and Hoff and Thompson[14] have attempted similar correlations in the heavy elements. Hoff, et al. used the more fundamental indication, the ft value, to determine the nature of the electron-capture transitions. However, Hoff was still somewhat limited by the lack of experimental data. Only a relatively few isotopes had been studied thoroughly enough so their complete decay schemes were known. Many other electron-capture nuclides whose decay schemes were not known were included under the assumption of ground state transitions. As pointed out by Hoff, such an assumption was obviously not

realistic, but no other method was available for treating the data.

In addition to the isotopes studied experimentally by the author, the electron-capture decay schemes of a number of electron-capture nuclides in the heavy element region have been studied recently. Some of the data used previously have subsequently been changed. Therefore, a new survey of these isotopes appears to be warranted. Since there is no basis for assuming ground state transitions in the unstudied isotopes, only those nuclides whose electron-capture decay schemes have been experimentally studied or can reasonably be inferred from the negatron or alpha decay to the same daughter nuclides are included. These nuclides together with their decay energies, partial half-lives, and log ft values are listed in Table XXI.

From these data, it is apparent that most of the nuclides can be considered as either allowed or first forbidden $\Delta I = 0, 1$ yes. While the Cm^{241} transitions have ft values which are large enough to suggest a $\Delta I = 2$, yes assignment, $\Delta I = 1$, yes is a preferable assignment. This point has been covered adequately by Hoff.[14] Only four transitions are apparently second forbidden or higher. This is not surprising since the precise amount of electron capture branching to various excited levels is often very difficult to determine, and the highly forbidden transitions would be masked by the predominant allowed decay.

A plot of the logarithm of the partial electron capture half-life versus the logarithm of the neutrino energy for the allowed transitions is shown in Fig. 22. Only those transitions of Table XXI which have log ft values less than 6.0 are considered allowed. At^{211} is an exception as discussed above. The limits on the neutrino energy indicate K and L electron-capture energies, the actual neutrino energy lying

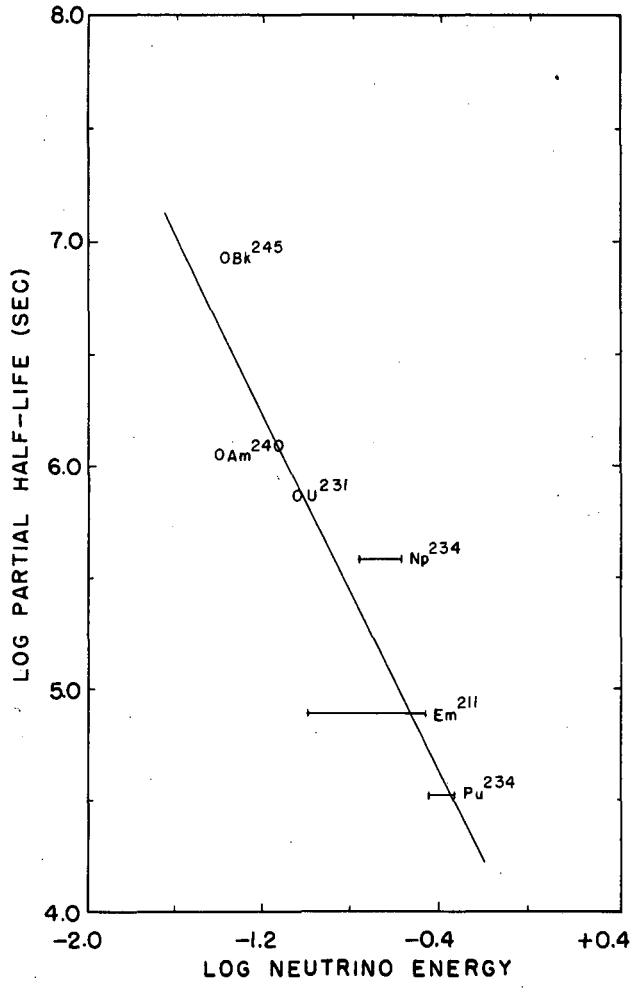


Fig. 22. Log of the partial electron capture half-life versus log of the neutrino energy for allowed electron capture.

Table XXI

Log ft Values for Nuclides Whose Electron Capture Decay Schemes are Known or Can be Inferred

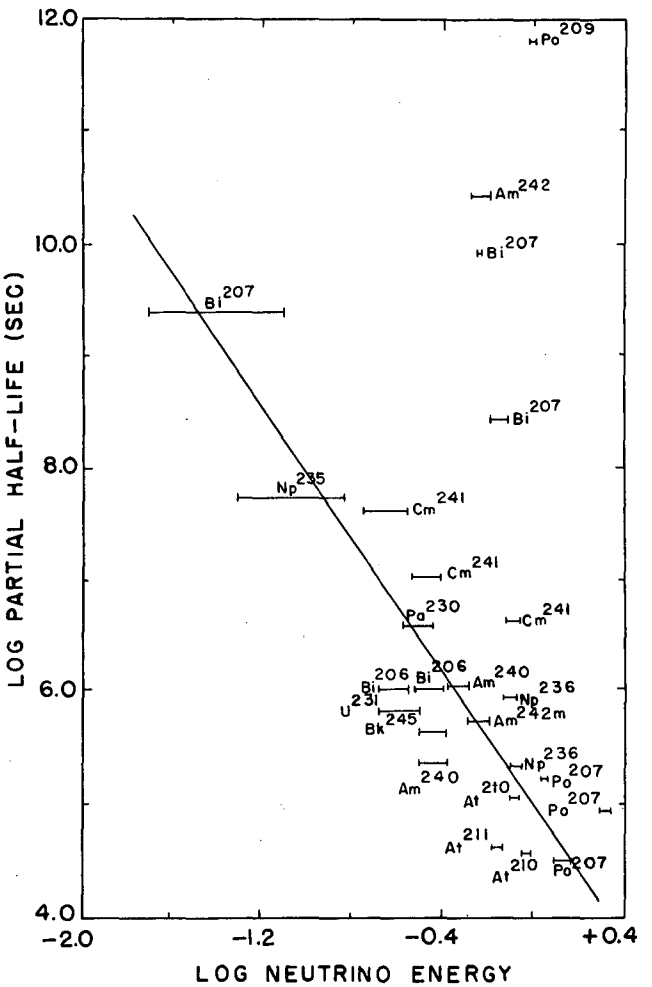
Isotope	Available energy from decay cycles (Mev)	Level to which decay proceeds (Mev)	Neutrino energy (limits allow for K and L electron capture) (Mev)	Partial electron capture half-life (seconds)	Log ft	Ref.
Bi^{206}	3.70	3.4 (50%)	0.21 - 0.285	1.1×10^{6}	6.3	58
		3.28 (50%)	0.33 - 0.405	1.1×10^{6}	6.6	
Bi^{207}	2.36	1.64 (87%)	0.63 - 0.76	2.9×10^{8}	9.6	59
		2.34 (10%)	0.02 - 0.08	2.5×10^{9}	8.0	
		0.57 (3%)	1.70 - 1.84	8.4×10^{9}	11.9	
Po^{207}	~3.1	1.74 (64%)	1.27 - 1.50	3.2×10^{4}	6.3	81
		1.00 (23%)	2.01 - 2.24	8.9×10^{4}	7.1	
		2.15 (12%)	0.86 - 1.09	1.7×10^{5}	6.7	
Po^{209}	1.93	0.90 (0.9-Mev level populated in 0.5% of total transitions)	0.94 - 1.01	6.3×10^{11}	13.3	93
At^{210}	3.93	2.92 (76%)	0.92 - 1.00	3.9×10^{4}	6.1	27
		3.04 (24%)	0.80 - 0.88	1.2×10^{5}	6.5	
At^{211}	0.76	ground state (no γ rays observed)	0.67 - 0.75	4.4×10^{4}	5.9	26, 81
Em^{211}	~2.6	2.49 (~100%)	0.1 - 0.35	7.7×10^{4}	5.6	81
Pa^{230}	1.32	0.94 (~100%) (γ ray observed)	0.27 - 0.36	4.1×10^{6}	7.5	17
U^{231}	0.34	0.23 (50%)	0.09	7.4×10^{5}	4.4	94
		ground state (50%) (decay of Th^{231})	0.23 - 0.32	7.4×10^{5}	6.1	

Isotope	Available energy from decay cycles (Mev)	Level to which decay proceeds (Mev)	Neutrino energy (limits allow for K and L electron capture)	Partial electron capture half-life (seconds)	Log ft	Ref.
Np^{234}	1.86	1.57 (γ ray observed)	0.17 - 0.27	3.8×10^5	5.9	26
Np^{235}	0.17	ground state (no γ rays observed)	0.05 - 0.15	3.54×10^7	7.2	14, 95
Np^{236}	0.91	0.04 (20%)	0.75 - 0.85	9.2×10^5	7.6	81
		ground state (80%)	0.79 - 0.89	2.3×10^5	7.0	
Pu^{234}	0.48	ground state (no γ rays observed)	0.36 - 0.47	3.4×10^4	5.6	14, 95
Am^{240}	1.46	1.02 (70%)	0.32 - 0.42	2.4×10^5	6.3	96
		1.40 (15%)	0.04	1.1×10^6	4.3	
		0.92 (14%)	0.42 - 0.52	1.2×10^6	7.3	
Am^{242}	0.65	0.04	0.49 - 0.59	2.7×10^{10}	11.7	17, 23
Am^{242m}	0.68	ground state (50%)	0.52 - 0.62	5.8×10^5	7.1	23
		0.04 (50%)	0.56 - 0.67	5.8×10^5	7.2	
Cm^{241}	0.89	ground state (65%)	0.76 - 0.87	4.7×10^6	8.4	96
		0.47 (28%)	0.29 - 0.40	1.1×10^7	8.0	
		0.59 (7%)	0.17 - 0.28	4.3×10^7	8.1	
Bk^{245}	0.70	0.26 (95%)	0.32 - 0.42	4.5×10^5	6.7	97
		0.64 (5%)	0.04	8.6×10^6	5.3	

somewhere between these limits, depending on the ratio of K and L electron capture. The theoretical expression for the probability of allowed electron capture predicts a slope of two for such a plot. A reference line has been drawn with the predicted slope. While the data are limited, only six transitions being classed as allowed, an approximate adherence to the theoretical slope is indicated.

A similar plot for the forbidden electron-capture transitions is shown in Fig. 23. Although no unique slope for this type of plot is predicted by theoretical considerations, the slope should be between two and three. The data fit a line of slope approximately three as indicated by the figure. Cm^{241} with its larger ft values and the very highly forbidden transitions of Bi^{207}, Po^{209}, and Am^{242} fall well away from the line.

It is quite apparent that a continuing program of the study of the electron-capture process in the heavy elements is succeeding in correlating electron-capture data with theoretical considerations. It is expected that further refinements of experimental data will bring about even better verification of the dependence of half-life on energy.



MU-10024

Fig. 23. Log of the partial electron capture half-life versus log of the neutrino energy for forbidden electron capture.

V. ACKNOWLEDGMENTS

I wish to express my gratitude to Professor G. T. Seaborg under whose direction these investigations were performed. The continued interest and helpful suggestions of Dr. S. G. Thompson are gratefully acknowledged. Helpful discussions with Professor J. O. Rasmussen, Jr. and Dr. R. A. Glass are sincerely appreciated. Discussions with and the assistance of Messrs. A. W. Stoner, J. P. Hummel, and Drs. W. G. Smith, F. S. Stephens, Jr., T. O. Passell, and H. Jaffe have been most helpful in many phases of the research.

The author also gratefully acknowledges the cooperation of Dr. J. G. Hamilton, G. B. Rossi, W. B. Jones, J. T. Vale, L. Houser, and the staffs of the 60-inch and 184-inch cyclotrons and the staff of the MTR reactor at the Reactor Testing Station, Arco, Idaho.

This work was performed under the auspices of the United States Atomic Energy Commission.

VI. REFERENCES

1. A. H. Compton and S. K. Allison, X-Rays in Theory and Experiment, D. Van Nostrand Company, Inc., New York, 1935. Second edition, p. 477 ff.
2. C. D. Broyles, D. A. Thomas, and S. K. Haynes, Phys. Rev. 89, 715 (1953).
3. L. S. Germain, Phys. Rev. 80, 937 (1950).
4. n = neutron
   p = proton
   e^- = negatron or negatively charged electron
   e^+ = positron or positively charged electron
   η = neutrino or antineutrino
5. R. J. Prestwood, H. L. Smith, C. I. Browne, and D. C. Hoffman, Phys. Rev. 98, 1324 (1955).
6. D. Maeder and P. Preiswerk, Phys. Rev. 84, 595 (1951).
7. C. E. Anderson, G. W. Wheeler, and W. W. Watson, Phys. Rev. 87, 668 (1952).
8. E. der Mateosian and A. Smith, Phys. Rev. 88, 1186 (1952).
9. I. Perlman, A. Ghiorso, and G. T. Seaborg, Phys. Rev. 77, 26 (1950).
10. I. Perlman and F. Asaro, Ann. Rev. Nuclear Sci. Vol. 4 (1954).
11. R. A. Glass, S. G. Thompson, and G. T. Seaborg, J. Inorg. and Nuclear Chem. 1, 3 (1955).
12. S. G. Thompson, Phys. Rev. 76, 319 (1949).
13. N. Feather, Proc. Roy. Soc. (Edinburgh) 63A, 242 (1952).
14. R. W. Hoff and S. G. Thompson, Phys. Rev. 96, 1350 (1954).
15. J. K. Major and L. C. Biedenharn, Revs. Modern Phys. 26, 321 (1954).

16. W. E. Nervik, private communication, reported by D. C. Dunlavey and G. T. Seaborg, Phys. Rev. 92, 206 (1953).

17. T. O. Passell, Ph. D. Thesis, University of California Radiation Laboratory Unclassified Report UCRL-2528 (March 30, 1954).

18. B. G. Harvey, private communication.

19. W. G. Smith, Ph. D. Thesis, University of California Radiation Laboratory Unclassified Report UCRL-2974 (June 1955).

20. E. L. Kelly and E. Segrè, Phys. Rev. 75, 995 (1949).

21. G. W. Barton, A. Ghiorso, and I. Perlman, Phys. Rev. 82, 13 (1951).

22. G. L. Johnson, R. F. Leininger, and E. Segrè, J. Chem. Phys. 17, 1 (1949).

23. H. Jaffe, Ph. D. Thesis, University of California Radiation Laboratory Unclassified Report UCRL-2573 (April 5, 1954).

24. F. F. Momyer, Ph. D. Thesis, University of California Radiation Laboratory Unclassified Report UCRL-2060 (February 1953).

25. F. F. Momyer, E. K. Hyde, A. Ghiorso, and W. E. Glenn, Phys. Rev. 86, 805 (1952).

26. R. W. Hoff, Ph. D. Thesis, University of California Radiation Laboratory Unclassified Report UCRL-2325 (September 1953).

27. J. W. Mihelich, A. W. Schardt, and E. Segrè, Phys. Rev. 95, 1508 (1954).

28. S. G. Thompson, A. Ghiorso, and G. T. Seaborg, Phys. Rev. 80, 781 (1950).

29. L. H. Treiman and M. H. Treiman, Los Alamos Scientific Laboratory Report LA-1403 (May 1952).

30. G. D. O'Kelley, Ph. D. Thesis, University of California Radiation Laboratory Unclassified Report UCRL-1243 (June 1951).

31. G. W. Barton, H. P. Robinson, and I. Perlman, Phys. Rev. 81, 208 (1951).

32. C. I. Browne, Ph. D. Thesis, University of California Radiation Laboratory Declassified Report UCRL-1764 (June 1952).

33. A. Ghiorso and A. E. Larsh, to be published.

34. F. S. Stephens, Jr., Ph. D. Thesis, University of California Radiation Laboratory Unclassified Report UCRL-2970 (June 1955).

35. A. Ghiorso, A. H. Jaffey, H. P. Robinson, and B. B. Weissbourd, National Nuclear Energy Series, Plutonium Project Record, The Transuranium Elements: Research Papers, McGraw-Hill Book Company, New York, 1949, Vol. 14B, 1226 (1949).

36. F. L. Reynolds, Rev. of Sci. Instr. 22, 749 (1951).

37. R. L. Graham, J. L. Wolfson, and R. E. Bell, Can. J. Phys. 30, 459 (1952).

38. I. Bergström and R. D. Hill, Arkiv för Fysik 8, 21 (1954).

39. R. D. Hill, E. L. Church, and J. W. Mihelich, Rev. of Sci. Instr. 23, 523 (1952).

40. D. R. Corson, K. R. MacKenzie, and E. Segrè, Phys. Rev. 57, 459, 1087 (1940).

41. H. M. Neumann and I. Perlman, Phys. Rev. 81, 958 (1951).

42. R. F. Leininger, E. Segrè, and F. N. Spiess, Phys. Rev. 82, 334 (1951).

43. Cheng, Rudulfo, Pool, and Kundu, Bull. Am. Phys. Soc. 29, No. 7, 16 (1954).

44. M. Mladjenovic and H. Slätis, Arkiv för Fysik, 9, No. 1, 41 (1955).

45. S. Rosenblum, M. Valadares, and M. Guillot, Compt. rend. 235, 238 (1952).

46. M.E. Rose and J.L. Jackson, Phys. Rev. 76, 1540 (1949).

47. D.A. Orth and G.D. O'Kelley, Phys. Rev. 82, 758 (1951).

48. R.A. James, A.E. Florin, H.H. Hopkins, Jr., and A. Ghiorso, National Nuclear Energy Series, Plutonium Project Record, The Transuranium Elements: Research Papers, McGraw-Hill Book Company, New York, 1949, Vol. 14B, 1604.

49. F. Asaro and I. Perlman, Phys. Rev. 88, 828 (1952).

50. G.D. O'Kelley, private communication (January 1954).

51. B.B. Kinsey, Can. J. Research 26A, 404 (1948).

52. A.H. Compton and S.K. Allison, op. cit. pp 640-644.

53. D.R. Corson, K.R. MacKenzie, and E. Segrè, Phys. Rev. 58, 672 (1940).

54. K.L. Hall and D.H. Templeton, unpublished data (August 1951).

55. D.H. Templeton, J.J. Howland, and I. Perlman, Phys. Rev. 72, 758 (1947).

56. D.G. Karraker, A. Ghiorso, and D.H. Templeton, Phys. Rev. 83, 390 (1951).

57. M.E. Rose, G.H. Goertzel, and C. Swift, privately circulated tables.

58. D.E. Alburger and M.H.L. Pryce, Phys. Rev. 95, 1482 (1954).

59. N.H. Lazon and E.D. Klema, Phys. Rev. 98, 710 (1955).

60. A.H. Wapstra, Thesis, University of Amsterdam, 1953 (unpublished).

61. A. W. Stoner and F. Asaro, unpublished data (May 1954).

62. G. W. Barton, Ph. D. Thesis, University of California Radiation Laboratory Unclassified Report UCRL-670 (May 1950).

63. R. W. Hoff, J. P. Hummel, and F. Asaro, private communication (June 1955).

64. W. J. Sturm and V. Johnson, Phys. Rev. 83, 542 (1951).

65. G. Wentzel, Z. Physik 43, 524 (1927).

66. N. F. Mott and I. N. Sneddon, Wave Mechanics and Its Applications, Oxford University Press, London, 1948, pp 338 ff.

67. E. H. S. Burhop, Proc. Roy. Soc. (London) A148, 272 (1935).

68. L. Pincherle, Nuovo cimento 12, 81 (1935).

69. H. W. S. Massey and E. H. S. Burhop, Proc. Roy. Soc. (London) A153, 661 (1936).

70. J. C. Slater, Phys. Rev. 36, 57 (1930).

71. E. Arends, Ann. Physik 22, 281 (1935).

72. I. Backhurst, Phil. Mag. 22, 737 (1936).

73. E. H. S. Burhop, The Auger Effect and Other Radiationless Transitions, Cambridge University Press, Cambridge, England, 1952, pp 44-51.

74. H. Tellez-Plascencia, J. phys. et radium 10, 14 (1949).

75. M. Ference, Phys. Rev. 51, 727 (1937).

76. J. Schooley, private communication (January 1955).

77. O. Huber, Humbel, Schneider, and Shalit, Helv. Phys. Acta 25, 3 (1952).

78. T. A. Johnson and J. S. Foster, Can. J. of Phys. 31, 464 (1953).

79. I. Bergström and S. Thulin, Phys. Rev. 79, 539 (1950).

80. T. Azuma, J. Phys. Soc. of Japan 9, 443 (1954).

81. Experiment results of author.

82. R. Steffens, Huber, and Humbel, Helv. Phys. Acta 22, 167 (1949).

83. B.B. Kinsey, Can. J. Research A26, 421 (1948), data of Ellis, Proc. Roy. Soc. (London) A139, 336 (1936).

84. B.B. Kinsey, Can. J. Research A26, 421 (1948), data of Flammersfeld, Z. Physik 114, 227 (1939).

85. J.W. Mihelich, Phys. Rev. 88, 415 (1952).

86. C.D. Ellis, Proc. Roy. Soc. (London) A138, 318 (1932); A143, 350 (1934).

87. E. Fermi, Z. Phys. 88, 161 (1934).

88. H.A. Bethe and R.F. Bacher, Revs. Modern Phys. 8, 82 (1936).

89. G. Gamow and E. Teller, Phys. Rev. 49, 895 (1936).

90. R.E. Marshak, Phys. Rev. 61, 431 (1942).

91. M.G. Mayer and J. Hans D. Jensen, Elementary Theory of Nuclear Shell Structure, John Wiley and Sons, New York, 1955, p. 154.

92. M. Goldhaber and A.W. Sunyar, Phys. Rev. 83, 906 (1951).

93. F. Asaro, private communication (June 1955).

94. M.S. Freedman, F. Wagner, Jr., A.H. Jaffey, and J. May, Phys. Rev. 86, 633 (1952).

95. R.W. Hoff, private communication (June 1955).

96. R.A. Glass, Ph.D. Thesis, University of California Radiation Laboratory Unclassified Report UCRL-2560 (April 1954).

97. F.S. Stephens and A. Chetham-Strode, private communication (July 1955).